R-10-45

FASTREACT – A streamline-based approach for the solution of multicomponent reactive transport problems

Paolo Trinchero, Jorge Molinero, Gabriela Román-Ross
Amphos[21] Consulting S.L

March 2014

Svensk Kärnbränslehantering AB
Swedish Nuclear Fuel
and Waste Management Co

Box 250, SE-101 24 Stockholm
Phone +46 8 459 84 00

ISSN 1402-3091
SKB R-10-45
ID 1391963

FASTREACT – A streamline-based approach for the solution of multicomponent reactive transport problems

Paolo Trinchero, Jorge Molinero, Gabriela Román-Ross
Amphos[21] Consulting S.L

March 2014

Abstract

Reactive transport models are powerful interdisciplinary tools that are commonly used to support decision and policy-making processes related to sensitive environmental issues. In the framework of safety assessment studies for nuclear fuel repositories, these types of models pose formidable computational challenges due to the non-linearity of the underlying system of equations as well as the very large spatial and temporal scales involved. It turns out that modelers are usually forced to oversimplify things either on the "hydrogeological" side or on the "chemical" aspects of the problem, or on both. In this work, we present a numerical framework, denoted as FASTREACT, for the efficient solution of large-scale reactive transport problems. The methodology is based on the theory of stochastic-convective or stochastic-advective(-reactive) models, which states that, assuming local-scale dispersion is neglected, geometrically complex configurations can be reduced to a set of streamlines that can be treated independently. Under these conditions and considering a chemically homogeneous medium with steady state flow conditions, the flux-averaged concentration at a given control location, or other quantities of interest, can be provided by one single reference simulation that incorporates explicitly all the relevant geochemical processes (e.g. mineral dissolution/precipitation, aluminosilicates weathering, cation exchange reactions, and aqueous redox reactions).

FASTREACT has been developed with safety assessment calculations of radionuclide transport in fractured rock in mind and thus provides efficient handling of the coupling between advection, reactions and exchange processes (i.e. matrix diffusion) for large amounts of input and output data. In the present work, the methodology is first tested using five heterogeneous conductivity fields where a "typical" transport problem, i.e. the migration and spread of a contaminant plume, is solved using FASTREACT. The results, in this case breakthrough curves of a conservative and a reactive solute at given control planes, are successfully compared with those obtained using a "standard" Eulerian approach, whereas the computational performance of FASTREACT is shown to be much more efficient when compared with the "traditional" Eulerian simulations. Finally a real-case application is presented where the evolution of the "background" geochemistry (excluding radionuclides) is simulated at a regional scale and over a very large time frame. The results show that the approach is able to capture the processes of main interest for the considered transport problem, i.e. advection through the fractures, key geochemical reactions and the retention effect of the matrix, and their interactions.

Contents

1 Introduction

1.1 Motivation

In the framework of safety assessment studies for geological disposal, large scale models are powerful inter-disciplinary tools aiming at supporting regulatory decision making as well as providing input for repository engineering activities. Striking aspects of these kinds of models are their very large temporal and spatial modelling scales (the former spanning from thousands of years up to one million years, the latter covering areas of several square kilometres) and the need to integrate different processes, which in turn take place over a multiplicity of different scales. It turns out that these kinds of models may be highly computationally demanding and sometimes even unfeasible.

This could be the case for reactive transport models, which need to simultaneously account for the effects of physical heterogeneity and complex nonlinear reactions (e.g. mineral dissolution and precipitation, adsorption and desorption, microbial reactions and redox transformations). This problem is usually overcome by adopting a compromise: either (1) defining simplified geometries (e.g. representative vertical cross-sections, in the best of the cases) with a detailed description of geochemical processes, or (2) carrying out complex three-dimensional flow models with simplified geochemical formulations (usually K_d-based). In this work, we present a Lagrangian-based framework that aims at solving multi-component-reactive transport problems with a computationally efficient approach where complex systems are reduced to sets of one-dimensional models.

1.2 Scope and objectives

This report provides a detailed account of the implementation, verification and application of a Lagrangian-based framework, denoted as FASTREACT (FrAmework for STochastic REACtive Transport), for the efficient solution of multicomponent reactive transport problems. The primary objectives of the work are to:

- Analyse the validity of the approach when applied to synthetic heterogeneous media (i.e. multi-Gaussian fields).
- Provide a qualitative evaluation of the implications of the underlying simplifications and assumptions on the results.
- Present a real case application where the adoption of the FASTREACT approximation allows implementation and computation of fully coupled reactive transport models at a regional scale.

2 Approach and underlying assumptions

2.1 Theoretical background

The FASTREACT approach is based on the theory of Stochastic-Convective (SC) models (Shapiro and Cvetkovic 1988). In most cases, these models rely on the assumption that local-scale dispersion can be neglected and flow is steady. Under these conditions, a geometrically complex transport problem can be reduced to a set of streamlines that in turn can be treated independently. Specifically, when transverse local dispersion is neglected, no mass exchange occurs between adjacent streamlines, which then can be handled separately in the transport model (see Figure 2-1).

SC models were originally used for the interpretation of in-situ conservative tracer tests. In this context, the breakthrough curve of the tracer, $C^f(t)$, can be described as a simple convolution of the inflow concentration $c^{in}(t)$, and the probability distribution function (PDF) of solute arrival times in the considered control plane, $p(\tau)$, see Shapiro and Cvetkovic (1988):

$$C^f(t) = \int_0^t c^{in}(\tau)\, p(t-\tau)\, d\tau \qquad 2\text{-}1$$

In this equation, τ is the advective travel time between the source and the control plane (Figure 2-1), and the PDF expresses the probability of travel time for transport of a conservative solute in the ensemble of flow paths connecting source and control plane. Depending on the application, the PDF can be obtained from numerical simulations, analytical approximations, or measured breakthrough curves.

This formulation is particularly attractive since the travel time PDF, also denoted as transfer function, can be inferred from a simple deconvolution. The information provided by this transfer function can then be used to get insight into key features of the medium such as its textural structure and heterogeneity in hydraulic properties, including the degree of preferential flow (e.g. Trinchero et al. 2011).

The intrinsic efficiency of stochastic-convective models (also referred to as stochastic-advective models) makes them particularly suitable for the solution of reactive transport problems. For these applications, solving a set of one-dimensional problems is in most cases computationally much less expensive than solving for transport in a single multidimensional system. Thus, the stochastic-convective framework of Shapiro and Cvetkovic (1988) was extended to reactive transport by Cvetkovic and Dagan (1994). This modelling approach was later to be referred to as the LaSAR approach (Lagrangian Stochastic Advective Reactive). Whereas the work by Cvetkovic and Dagan (1994) considered linear reactions only, e.g. linear equilibrium sorption and first-order sorption kinetics, Dagan and Cvetkovic (1996) extended the LaSAR approach further to non-linear processes (such as sorption according to the non-linear Langmuir isotherm model).

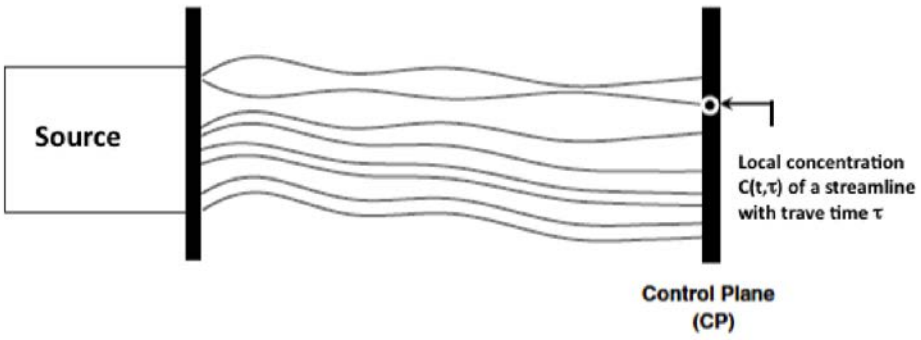

Figure 2-1. *Schematic representation of a transport problem decomposed into a set of independent streamlines (modified from Malmström et al. 2008).*

In the past years, many other efforts have been made to generalise and extend the framework of SC models to the solution of reactive transport problems (e.g. van der Zee and Van Riemsdijk 1987, Simmons et al. 1995, Berglund and Cvetkovic 1996, Cirpka and Kitanidis 2000). Most of these works provide efficient formulations for the analysis of breakthrough curves and/or temporal moments spatially integrated over given control planes. In this case, the reactive breakthrough curve for the set of streamlines can be obtained by integrating over all arrival times weighted by their probability:

$$C_k^f(t) = \int_0^\infty c_k(t,\tau)p(\tau)d\tau \qquad 2\text{-}2$$

where $C_k^f(t)$ is the concentration of compound *k* averaged over the outflow of the domain and $c_k(t,\tau)$ is the concentration associated with a single streamline of arrival time τ in the considered control plane.

The model development briefly outlined above goes from conservative/non-reactive models via models that consider linear processes to those handling also non-linear reactions. However, it should be noted that in most of the papers cited above chemistry is reduced to relatively simple reactions (e.g. bimolecular reactions or linear sorption). As a further development of these stochastic advective-reactive transport models, Malmström et al. (2004) presented a framework where reactive transport problems were studied using a numerical tool for modelling the chemical reactions.

Specifically, Malmström et al. (2004) used parametric transfer functions coupled to a PHREEQC (Parkhurst and Appelo 1999) reference simulation to compute the first and second temporal moments of relevant parameters (i.e. pH and Mg, SO_4^{2-} and Zn concentrations) at a control plane. This modelling approach was referred to as LaSAR-PHREEQC. Malmström et al. (2004) used spreading of acid mine drainage as example application. LaSAR-PHREEQC modelling of acid mine drainage was presented also in a later study by Malmström et al. (2008), who, among other things, investigated the effects of spatial variability in both travel time and chemical parameters.

2.2 Methodological approach and fields of application

The proposed methodology, denoted as FASTREACT, aims at providing a tool for the efficient solution of a wide range of reactive transport problems. As such, FASTREACT is intended to be a numerical framework rather than a new mathematical development, within which complex reactive transport modelling can be carried out by applying the following stepwise approach:

Step 1. Collection of information on advective transport, i.e. solute travel times, associated with one or multiple sets of streamlines in the transport domain of interest, and formulation of travel time PDFs.

Step 2. Parameterisation and calculation of one or several one-dimensional reference reactive transport simulations.

Step 3. Modelling of reactive transport by coupling the reactive reference simulation(s) and travel times along the considered set(s) of streamlines.

It is worth noting that the approach described above, which is illustrated in Figure 2-2, is similar to that of LaSAR-PHREEQC proposed by Malmström et al. (2004). Thus, there are no differences between FASTREACT and LaSAR-PHREEQC, as presented by Malmström et al. (2004), in terms of principles, potential fields of application, input data that can be handled, or process models that can be used. Instead, FASTREACT should be viewed as tool for modelling reactive transport according to the LaSAR-PHREEQC concept.

In particular, FASTREACT has been developed with safety assessment calculations of radionuclide transport in fractured rock in mind. It provides efficient handling of the coupling between advection (represented by travel time distributions, which usually are obtained from particle tracking simulations rather than being based on parametric functions) and reactions (PHREEQC, or any other available geochemical code) for large amounts of input and output data, such as those arising when using travel time distributions obtained from numerical simulations in multiple realisations of stochastic fields. Furthermore, in FASTREACT exchange of mass between a mobile zone (i.e. the fracture) and the matrix can be explicitly accounted for.

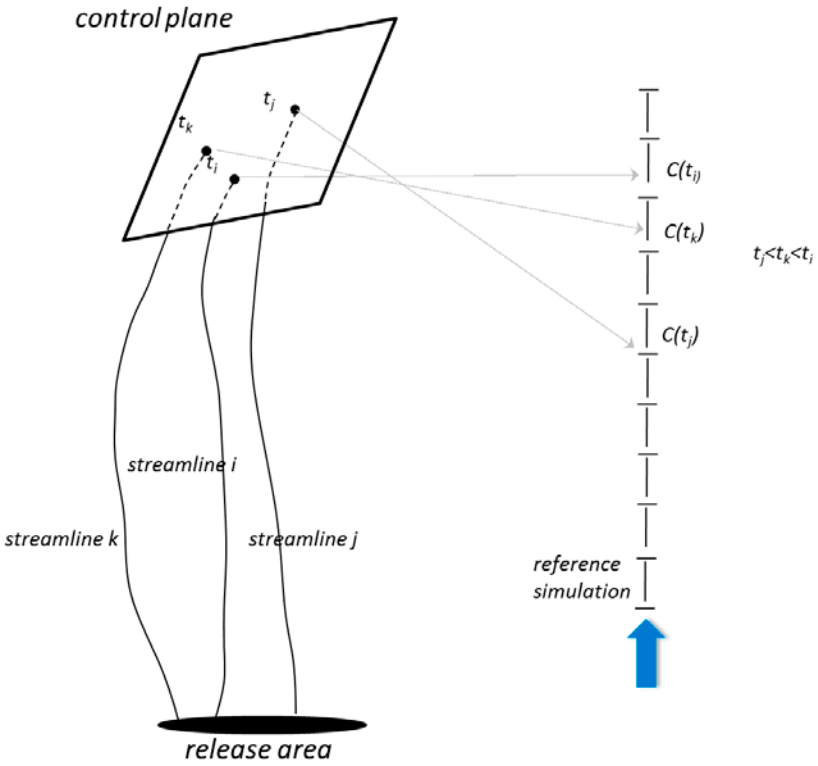

Figure 2-2. *Illustrative sketch showing the use of FASTREACT to provide maps of concentrations at the intersection between the ensemble of streamlines and a given control plane.*

Capabilities for handling multiple realisations are important in safety assessment applications. The transport between fractures and the surrounding rock matrix (where there is no groundwater flow), and the continued transport in the rock matrix need to be considered when modelling transport in fractured rock. Therefore, a simplified treatment of matrix diffusion is included in the current version of FASTREACT (Section 4.5.3), which is another development of FASTREACT that makes useful for safety assessment modelling.

The range of applicability of FASTREACT is broad and includes the modelling of radionuclide migration, the evaluation of the hydrochemical evolution of a given subsurface volume and the simulation of the fate and transport of contaminant plumes. Nevertheless, the applicability of the methodology is indissolubly linked to the underlying simplifying assumptions and thus is problem-specific (see Section 2.4 for further details).

Concerning applications, it should be noted that one important original motivation for developing FASTREACT was to enable process-based calculations of "equivalent K_d-values" for safety assessment purposes. This would imply reactive transport modelling with process models in PHREEQC (or any other suitable geochemical code) for the specific retention processes thought to be of importance for the various combinations of radionuclides, groundwater compositions and bedrock and fracture mineralogical conditions considered in the safety assessment.

Breakthrough curves from modelling with combinations of such reaction models and relevant travel time distributions could then be interpreted in terms of K_d- values, i.e. the linear equilibrium sorption parameters that are used in safety assessment transport models, thereby lending support and providing complementary information to the empirically based K_d-values otherwise used. Although this particular application is not further discussed in the present report, it remains an important future application for FASTREACT and a motivation for continued development.

2.3 Introduction to application example

This section provides an introduction to the application example presented in Section 4, thereby giving an early illustration of the modelling approach and an application. It should be noted that this is just one out of many possible model applications; the fact that we focus on this particular application does not mean that this is the only type of problem that can be modelled. In this FASTREACT application, travel times are explicitly assimilated from sets of streamlines computed by external hydrogeological simulators. These travel times are then used to provide time-variable maps of concentration at given control planes/control volumes. Thus, the current example deals with spatial distributions of concentrations, rather than spatially averaged temporal moments of breakthrough curves.

We summarise here the steps required to apply FASTREACT to the modelling of the hydrochemical evolution at a control plane located at the depth of a repository. A detailed presentation, including example results, is given in Section 4. The conceptual model assumes that the hydrochemical evolution of the groundwater at the selected control plane is the result of infiltration processes from the surface of the domain to the repository. In a fractured rock system, these infiltration processes occur in a network of preferential flow paths. Thus, one can roughly say that different portions of the plane are affected by different flow paths that in turn can be treated independently.

The first step of the modelling exercise requires the delineation of a representative number of recharge paths. This is usually done using particle tracking simulations; first the control plane is subdivided into a number of equal-sized cells, and second one particle is injected in the centre of each cell and backtracked to the surface (Figure 2-3). Each cell is thus characterised by a travel time, i.e. the time of travel from the surface to the corresponding cell location.

The travel time of the set of recharge paths is then used to parameterise a 1D reactive transport simulation (Figure 2-2). Finally, the related node of the reference simulation is used to provide the value of each geochemical variable (e.g. aqueous concentrations, Eh, pH, and mineral amounts) in each cell at repository depth (Figure 2-4; see Section 3.3.3 for details on the numerical approach).

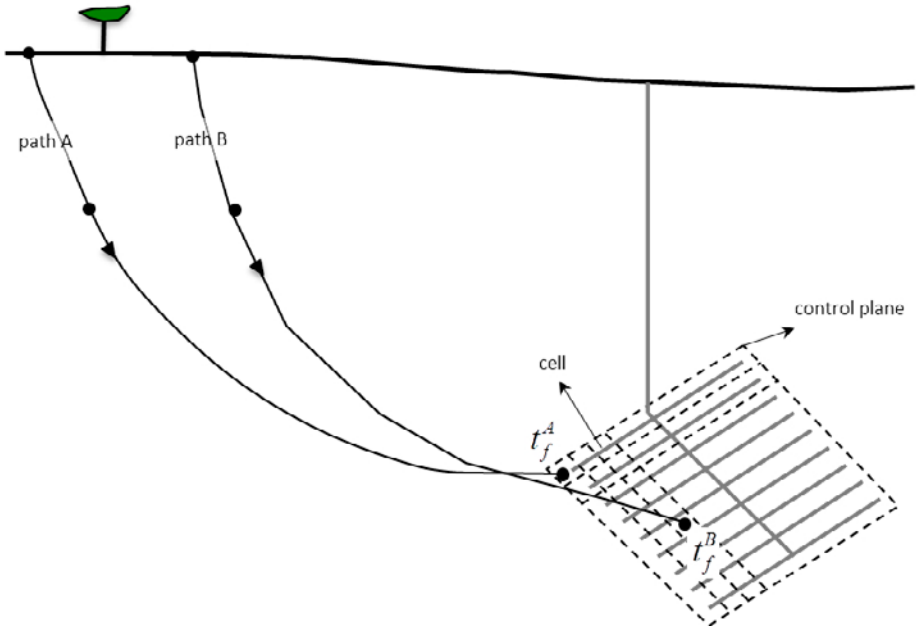

Figure 2-3. *Delineation of two recharge paths associated to different cells in the control plane.*

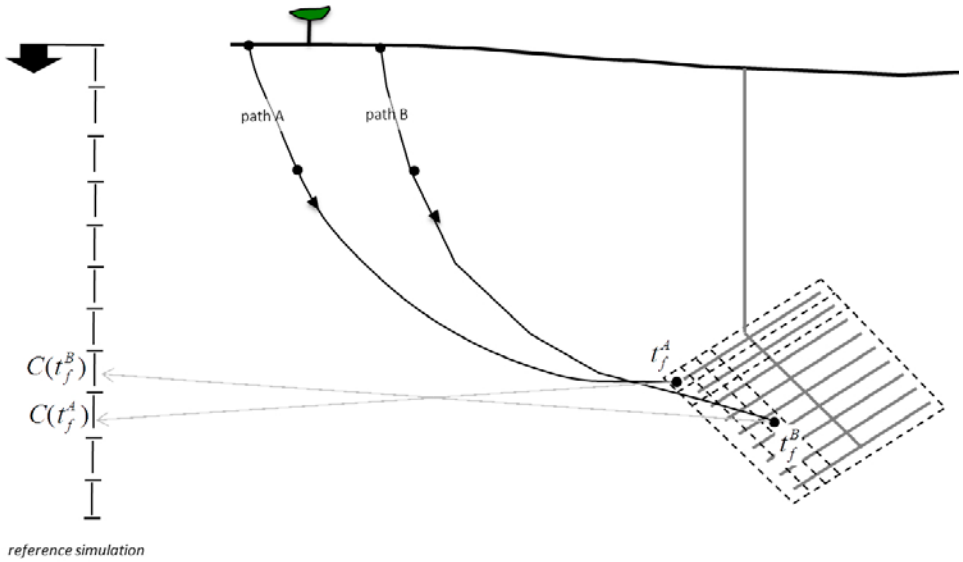

Figure 2-4. *The concentration in a given cell in the control plane is provided by the grid cell of the reference simulation having the same travel time.*

2.4 Implications of simplifying assumptions

The streamline approach presented in this work relies on three main simplifying assumptions: (i) the velocity field is steady (i.e. the streamlines do not change with time), (ii) the medium is chemically homogeneous with uniform initial conditions and (iii) mass exchange between streamlines is neglected.

The fulfilment of the first two assumptions is site-specific and depends on the hydrological and hydrochemical conditions of the system, including their temporal variability. In particular, the second assumption may have relevant implications for many Fennoscandian sites where groundwater is stratified according to different physico-chemical factors and water salinity increases with depth. In Section 4.5.1, we show and discuss a conceptual approximation that allows relaxing this hypothesis and defining heterogeneous initial conditions.

The third assumption has more subtle implications for key transport processes such as mixing. As shown by Kitanidis (1994), while solute spreading is produced by the spatial velocity variability, mixing is triggered by the combined effect of heterogeneity and local scale dispersion. In particular, due to the relatively small magnitude of local scale dispersion, mixing occurs in a very narrow zone located along the irregular edges of the contaminant plume (Oya and Valocchi 1998). Several works have investigated the effects of transverse mixing in rivers (Aucour et al. 2003), stream-aquifer interaction (Tonkin et al. 2002), saltwater intrusion (Sanford and Konikow 1989, Abarca et al. 2007), microbial reactions (Chu et al. 2005, Knutson et al. 2005) and heterogeneous aquifers (Zavala-Sanchez et al. 2009, and references therein).

The Peclet number is commonly used to quantify the relation between advection and local dispersion, and hence is a measure of the relative importance of dispersion. It is defined as $Pe = U \cdot I_Y / D$, where U is the mean groundwater velocity, I_Y is the correlation length of ln(K) (or some other characteristic length) and D is the local dispersion coefficient. It follows that Pe is inversely related to D. It turns out that the proposed methodology is particularly suited to advection-dominated problems (i.e. high Peclet numbers), while its applicability for problems where local scale dispersion is dominant (i.e. low Peclet numbers) needs to be investigated on a case-by-case basis.

In the specific case of modelling transport in fractured media, which is one potentially important use of the FASTREACT tool, flow is generally channelised, i.e. goes primarily through a network of preferential flow paths. Transport is usually advection-dominated while mixing processes occur as a result of mass exchange between the mobile regions (i.e. fractures and deformation zones) and the rock matrix. This makes FASTREACT particularly attractive for the simulation of large-scale reactive transport models in these kinds of media due to its numerical efficiency.

3 Testing and verification of FASTREACT

3.1 General approach

The FASTREACT methodology has been tested against a number of "synthetic solutions" computed using a set of heterogeneous continuous porous media. The approach for the testing and verification exercise has followed a number of steps that are illustrated in Figure 3-1 and summarised in the following description.

Step 1. **Generation of heterogeneous conductivity fields.** A set of equiprobable multi-Gaussian hydraulic conductivity fields has been generated using sequential Gaussian simulations. These fields are representative of moderately heterogeneous continuous porous media.

Step 2. **Definition of the transport problem.** A transport problem has been defined as consisting in the displacement of a solute plume from the left to right boundary of the domain (the details of the numerical setup are explained in Section 3.2.1). The transport problem has been solved for both a conservative solute and a reactive species (i.e. Strontium) that undergoes ion exchange reactions and precipitation processes (the details of the geochemical conceptual model are presented in Section 3.4).

Step 3. **Generation of the "synthetic solutions".** The transport problem defined in step 2 has been solved for the set of the conductivity fields generated in step 1 adopting a "standard" Eulerian approach. The solutions obtained with this approach (i.e. breakthrough curves at given control planes) have been treated as "synthetic solutions" against which to compare the results provided by the FASTREACT approach.

Step 4. **Lagrangian simulations.** Random walk particle tracking simulations (RWPT) have been performed in the set of conductivity fields (step 1).

Step 5. **FASTREACT approach.** For each of the conductivity fields (step 1), a reference PHREEQC one-dimensional simulation has been defined and used to map the entire set of particle trajectories at the considered control planes.

Step 6. **Comparison of non-reactive transport results (particle tracking vs. FASTREACT).** A verification of the implementation of the FASTREACT approach has been carried out. To this aim, breakthrough curves of a conservative solute have been computed along a selected control plane using the results of the random walk simulations. These breakthrough curves have then been compared with those obtained using FASTREACT.

Step 7. **Comparison of reactive transport results (Eulerian vs. FASTREACT).** Breakthrough curves averaged along the selected control planes have been computed using FASTREACT and compared with the synthetic solutions generated in step 3.

3.2 Case description

3.2.1 Geometry and parameterisation

The setup of the numerical simulations used in this study is shown in Figure 3-2 and consists of a rectangular domain of size L_x x L_y ($L_x=60L$, where L is a characteristic length, and $L_y/L_x=0.66$). No-flow boundary conditions are imposed along the upper and lower boundaries whereas constant heads, H_1 and H_2 ($H_1–H_2=1L$), are imposed along the left and right boundaries. A prescribed concentration ($C_0 \neq 0$) is set along a line of length L_{inj} ($L_{inj}/L_y=0.25$) coinciding with the position of the left boundary. The porosity and the longitudinal and transverse dispersivities have been assumed to be constant and set equal to 0.1, 0.2 L and 0.04 L respectively.

Average breakthrough curves are computed at a control plane (CP1) located at a distance $d=L_x/2$ from the left boundary. Two additional control planes, CP2 and CP3, are placed at $d=L_x/3$ and $d=L_x/6$, respectively, in order to investigate possible effects of the correlation scale of the heterogeneous fields on the results (Figure 3-3).

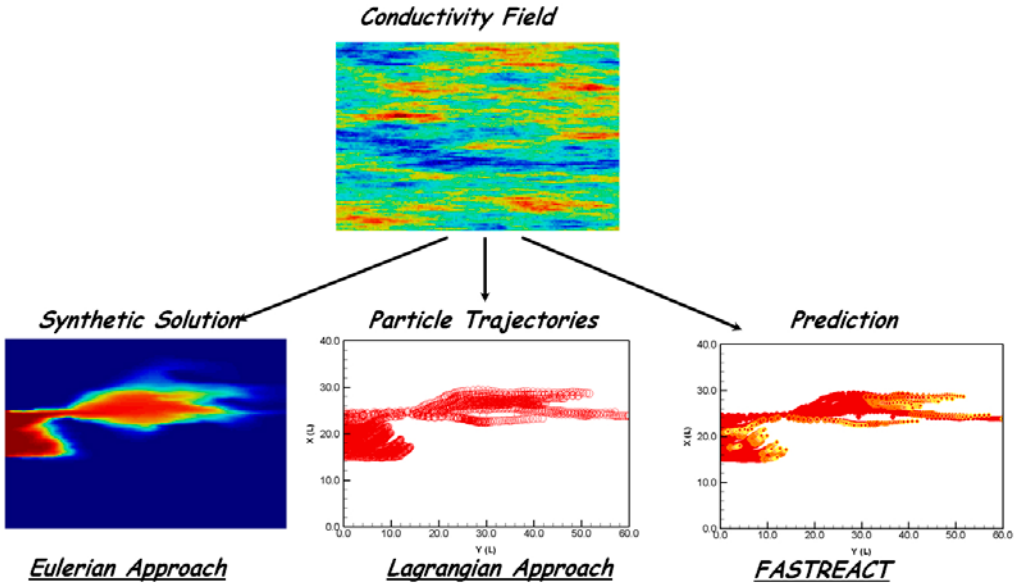

Figure 3-1. *Illustrative sketch of the approach used in the performance assessment of the FASTREACT methodology. The FASTREACT modelling also includes a 1D PHREEQC reactive transport model (not shown) providing the concentrations to be mapped in the considered control planes.*

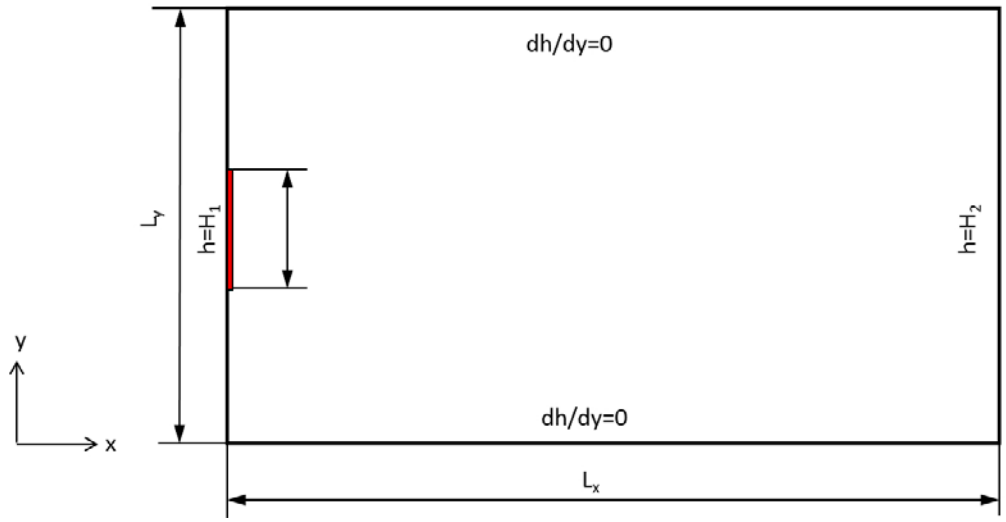

Figure 3-2. *Sketch of the model setup for flow and transport simulations.*

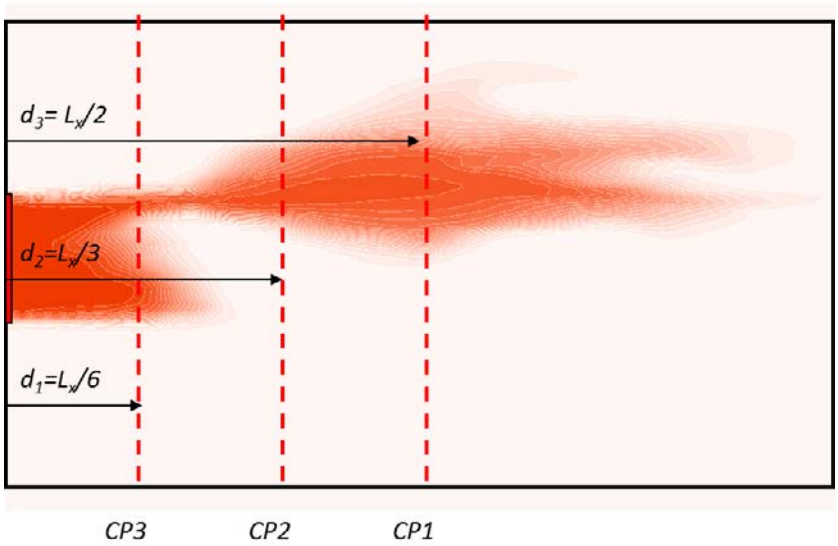

Figure 3-3. *Control planes considered in the computation of breakthrough curves.*

3.2.2 Heterogeneous conductivity fields

We have used five different randomly generated "synthetic fields" where the natural logarithm of hydraulic conductivity ($Y = ln(K)$) has been modelled as a multivariate Gaussian spatial random function with an exponential semi-variogram with mean $m_Y = 0$ (i.e. the K has a geometric mean $K_G = 1$ L/T), variance $\sigma_Y^2 = 2$, and integral scale $I = 10\ L$. The five realisations of random fields presented in Figure 3-4 were generated using the sequential Gaussian simulation program SGSIM (Deutsch and Journel 1998).

It is worth noting that the integral scale used for field generation is relatively large if compared with the domain size. It turns out that the statistics of the different realisations may in some cases differ from the underlying geostatistical model (Table 3-1).

Table 3-1. Statistics, i.e. mean (m_Y) and variance (σ_Y^2) of Y = ln K, for the five considered realisations, generated using $m_Y = 0$ and $\sigma_Y^2 = 2$.

Realisation	m_y	σ_Y^2
F1	0.27	2.09
F2	0.01	1.87
F3	0.17	2.23
F4	–0.10	2.00
F5	0.07	1.58

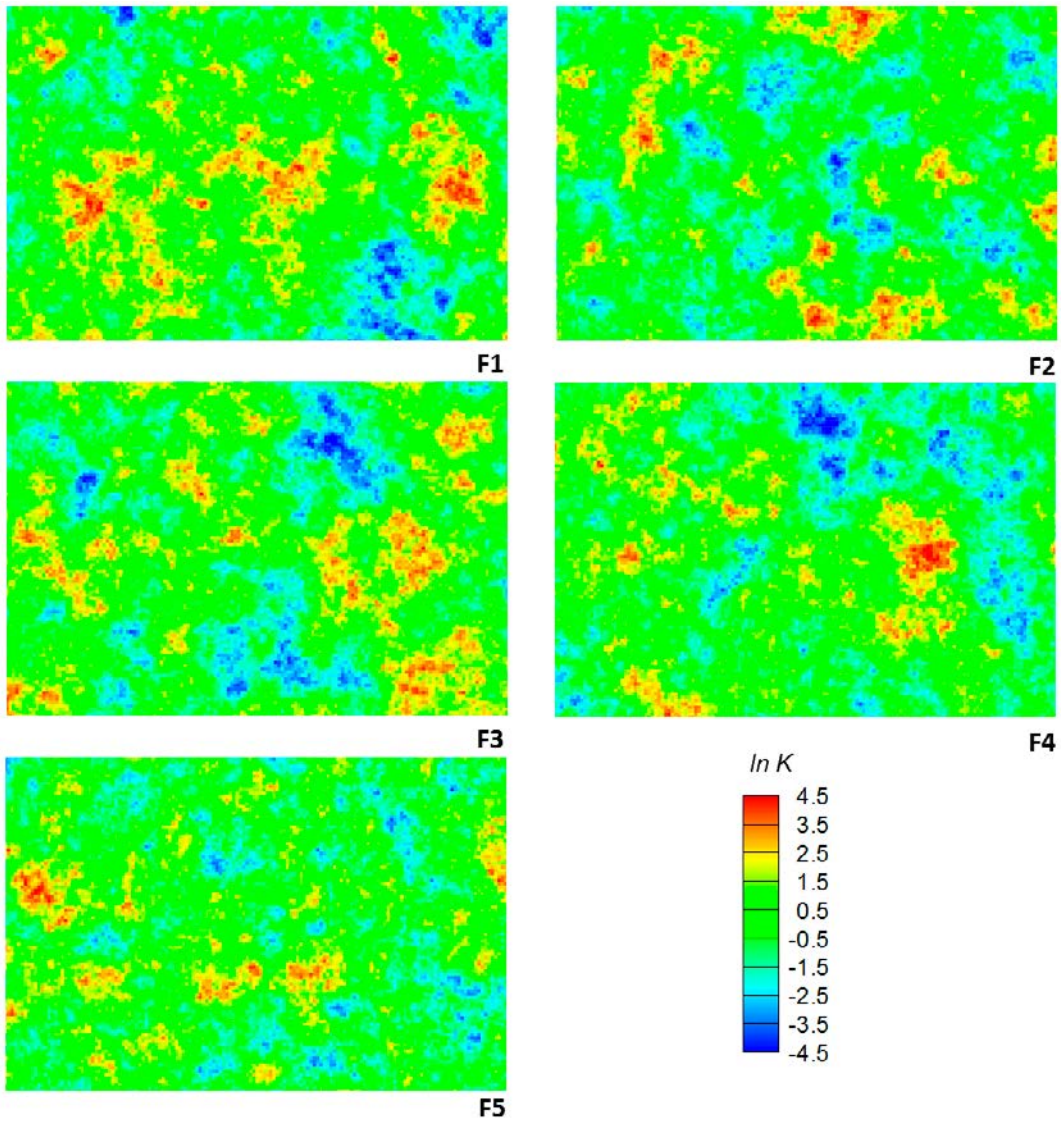

Figure 3-4. *The five realisations of the multivariate Gaussian log-conductivity fields used in the numerical simulations.*

3.3 Numerical approaches

3.3.1 Eulerian approach

The "synthetic solutions" have been computed using the reactive-transport simulator PHAST (Parkhurst et al. 2004). The model domain (Figure 3-2) has been discretised into 15,000 uniform grid cells, each with the size $0.4L \times 0.4L$. A constant concentration of a conservative and a reactive (i.e. Strontium) solute is associated to the injection line (see Figure 3-2). The retention processes implemented in the geochemical model are explained in detail in Section 3.4.

The flux-averaged concentrations (e.g. Parker and van Genuchten 1984) at the three control planes (CP1, CP2 and CP3) are computed as follows:

$$C^f(t) = \frac{\sum_{i=1}^{n} c_i(t) \cdot q_i}{Q} \qquad 3\text{-}1$$

where c_i is the concentration at the node of the i:th cell of the control plane, q_i is the flow perpendicular to the control plane that crosses the side of the same cell and Q is the total flow crossing the control plane.

3.3.2 Lagrangian approach

First, steady-state flow is simulated using the code MODFLOW2000 (Harbaugh et al. 2000). For the sake of consistency, the discretisation of the domain is the same as that used in the Eulerian model (i.e. PHAST). The resulting velocity fields are used to simulate solute transport, which is solved using the random walk particle tracking code RW3D (Fernàndez-Garcia et al. 2005). For each realisation, 200 particles are injected proportionally to the flux. Purely advective transport simulations allow delineating the set of trajectories from the injection area to the considered CPs.

An illustrative plot of the effect of heterogeneity on the groundwater head and the related advective particle tracking simulations is shown in Figure 3-5 for field F1 and F2. It is interesting to note that, although the two fields are two realisations of the same random function, the results of the particle tracking simulations are very different. In field F1, most of the particles have travelled a distance greater than half of the domain length after 120 time units, while particle velocities generally are considerably lower in field F2. The reason for this difference in behaviour is related to the large integral scale used compared to the domain size. This results in (I) conductivity fields whose statistics may differ substantially from the underlying geostatistical model (see Table 3-1) and (II) transport conditions that are far from being ergodic (i.e. the whole statistical variability is not "sampled" in a single transport simulation).

In order to recover conservative breakthrough curves at the considered control planes from the particle tracking simulations, it should be considered that these simulations produce discrete distributions of sub-ensembles of mass (particles). Thus, these discrete distributions have to be converted to a continuous distribution of concentrations.

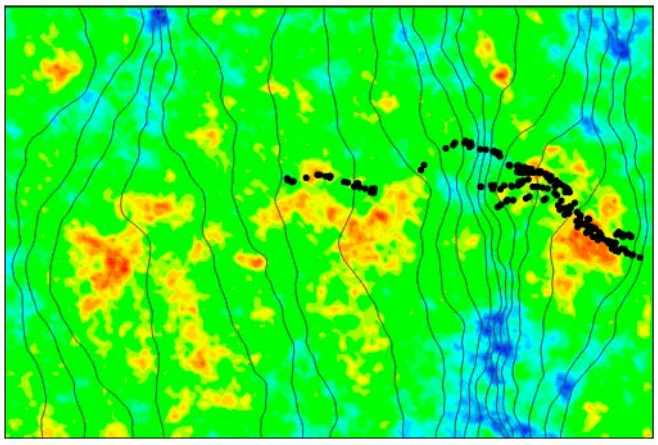

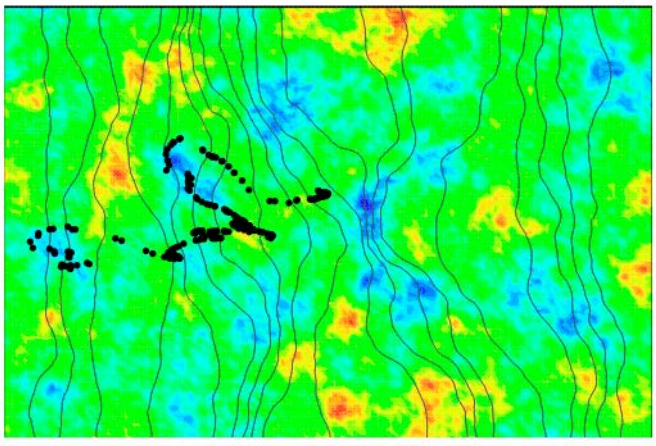

Figure 3-5. *Isolines and position of the injected particles after 120 time units for realisation F1 (a) and F2 (b).*

A commonly used estimate of the normalised flux-averaged concentration at a given control plane is given by the following probability density function (PDF):

$$p(t_j) \approx \frac{1}{M_a} \sum_p \frac{m_p I\{T_p \in B_j\}}{\Delta t_j} \qquad 3\text{-}2$$

where m_p is the mass associated to each particle, M_a is the total mass injected, t_j denotes the centroid of the j:th discretisation element in time with size Δt_j, T_p is the passage time of the p:th particle, B_i is the considered time interval and $I\{\cdot\}$ is an indicator function defined as

$$I\{t \in B\} = \begin{cases} 1 & t \in B \\ 0 & otherwise \end{cases} \qquad 3\text{-}3$$

Due to the difficulty of inferring a PDF from a discrete distribution of particles, the breakthrough curve of a continuous mass injection (like the one used in this modelling work) is usually inferred as the cumulative density function (CDF) of a pulse of concentration injected at time zero:

$$P(t) = \int_0^t p(\tau) d\tau \qquad 3\text{-}4$$

This CDF is usually evaluated numerically as:

$$P(t_j) \approx \frac{1}{M_a} \sum_p m_p \cdot \gamma(T_p \in C_j) \qquad 3\text{-}5$$

where $\gamma(\cdot)$ is an indicator function defined as:

$$\gamma\{t \in C\} = \begin{cases} 1 & t \in C \\ 0 & otherwise \end{cases} \qquad 3\text{-}6$$

and C is the time interval spanning from zero to t.

3.3.3 FASTREACT approach

As explained in section 3.3.2, a number of particles (in this case 200 particles) are injected proportionally to the flux within the injection zone in each Lagrangian simulation. This means that each particle is implicitly associated with a constant amount of flow, equal to Q_{inj}/n_p, where Q_{inj} is the total flow through the injection zone and n_p is the number of particles. Using a summation over all injected particles, Equation 3-1 can be evaluated numerically as:

$$C^f(t) = \frac{Q_{inj}}{n_p Q} \sum_{i=1}^{n_p} c_i(t, \tau_i) \qquad 3\text{-}7$$

where c_i is the concentration at the intersection between the streamtube associated with the i:th particle and the control plane, and τ_i is the travel time of the i:th particle from the injection zone to the control plane. The flux-weighting of concentrations indicated in Equation 3-1 is obtained through the non-uniform, flux-proportional distribution of particles among the nodes in the injection zone, implying that more particles enter at nodes where the flow velocity is high.

As described in Section 2.2, the concentration of the whole set of streamtubes is provided by one single reference simulation. This simulation is carried out over a one-dimensional domain that is discretised into N nodes each of them having a related residence time expressed as:

$$\tau_j^{RS} = \frac{d_j}{v} \qquad 3\text{-}8$$

where v is the advective groundwater velocity in the reference simulation and d_j is the distance of the j:th node from the inlet boundary. It turns out that in Equation 3-7, the travel time of the i:th streamtube is approximated as:

$$\tau_i = \tau_k^{RS} \mid \left(\tau_k^{RS} - \tau_i\right) = \min\left(abs\left(\tau_k^{RS} - \tau_i\right)\right) \qquad 3\text{-}9$$

Another way of seeing Equation 3-7 is as a numerical integration of Equation 2-2 and thus, given the approximation of Equation 3-9, it can be rewritten as:

$$C^f(t) = \frac{Q_{inj}}{Q} \sum_{k=1}^{N} c\left(t, \tau_k^{RS}\right) p\left(\tau_k^{RS}\right) \Delta\tau \qquad 3\text{-}10$$

where $p\left(\tau_k^{RS}\right)$ is the discrete travel time PDF of the ensemble of streamlines, which is described using the time bin-width, $\Delta\tau$, of the reference simulation (see Figure 3-6). Thus, in this case the summation/numerical integration is over the nodes in the 1D reactive transport reference simulation, and the flux-weighting of concentrations is included through the travel time PDF. Note that the calculation in Equation 3-10 needs to be repeated for every aqueous component to be studied in the reactive transport modelling.

This expression is particularly interesting as it provides some information regarding the parameterisation of the reference simulation (Step 2 in Section 2.2). In fact, as illustratively shown in Figure 3-6, $\Delta\tau$ in Equation 3-10 depends on the spatial discretisation of this reference simulation; a "fine" discretisation (i.e. short $\Delta\tau$) provides a good approximation of an underlying continuous ("smooth") travel time PDF, whereas a "coarse" one implies larger errors relative to this underlying PDF.

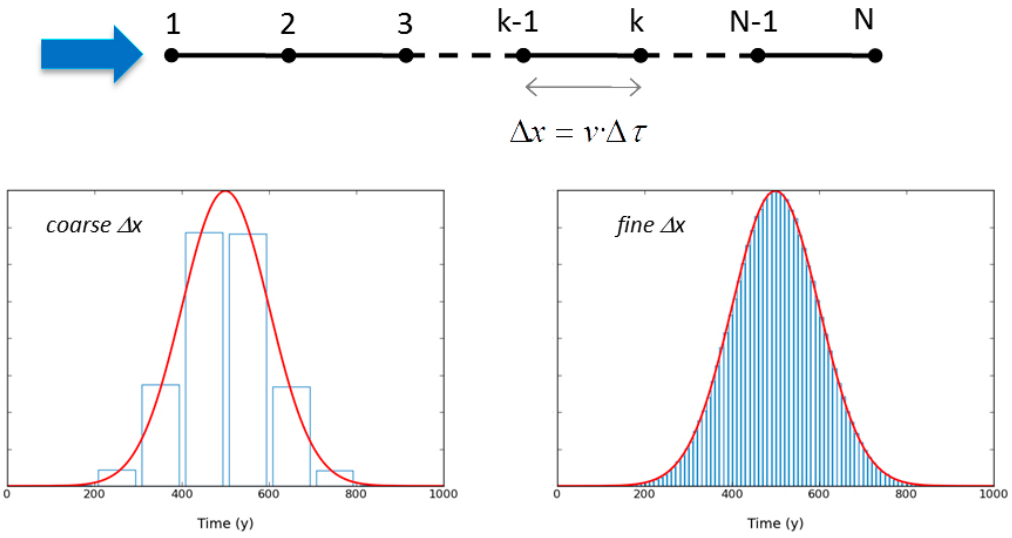

Figure 3-6. *A reference 1D simulation, with constant velocity, v, and constant grid size, Δx, is defined and used in FASTREACT (top). Depending on its discretisation, the travel time PDF of the considered set of streamlines (red line – bottom) is poorly approximated (bars – bottom left) or well represented (bars – bottom right).*

3.4 Geochemical system

The composition of the initial groundwater is the same as used by Piqué et al. (2010) to model the Forsmark deep groundwater conditions before repository release and is summarised in Table 3-1. The composition of the injection water is the same as the initial composition, except for the input of a conservative solute and a high strontium concentration ([Sr]=1.56×10^{-3} mol L^{-1}).

The reactive solute considered in the numerical exercise is strontium. The possible retention processes are the precipitation of the $(Ca,Sr)CO_3$ solid solution and the sorption of Sr on illite cation exchange sites. The $(Ca, Sr)CO_3$ solid solution series is highly non-ideal, i.e., the activity coefficients of the end-members are not equal to 1. Since ternary non-ideal solid solutions [$(Ca,Sr)CO_3$] cannot be modelled with PHAST, conditional solubility constants have been considered for the strontianite end-members in order to take this non-ideality into account (see Grandia et al. 2007 for details).

Strontium can be exchanged in the planar type sorption sites of Illite (Bradbury and Baeyens 2000). The Gaines-Thomas selectivity coefficient has been obtained from Brouwer et al. (1983) (Table 3-2) and the total number of available planar sites is 0.0045 mol L^{-1} (see Table 3-3).

Table 3-1. Initial composition of groundwater (concentrations in mol L^{-1}).

	Deep GW (before repository release)
pH	6.84
pe	–2.63
Na	6.13×10^{-2}
K	8.00×10^{-4}
Ca	1.82×10^{-2}
Mg	4.73×10^{-3}
Sr	6.94×10^{-5}
P	6.46×10^{-8}
S	2.21×10^{-3}
Si	5.63×10^{-4}
Ba	2.21×10^{-3}
C	4.82×10^{-3}
Cl	1.01×10^{-1}
Cs	3.65×10^{-9}
Fe	5.80×10^{-5}
NH_4^+	7.28×10^{-5}

Table 3-2. Cation exchange reactions and Gaines-Thomas selectivity coefficients.

Reaction	Log K (25ºC)	Reference
Planar sites		
$X^- + Na^+ \leftrightarrow NaX$	0.0	(1)
$X^- + K^+ \leftrightarrow KX$	1.1	(1)
$X^- + Cs^+ \leftrightarrow CsX$	1.6	(1)
$2X^- + Sr^{2+} \leftrightarrow SrX_2$	1.13	(2)
$2X^- + Ca^{2+} \leftrightarrow CaX_2$	1.13	(2)
$2X^- + Mg^{2+} \leftrightarrow MgX_2$	1.13 (a)	
Type II sites		
$X^{II-} + Na^+ \leftrightarrow NaX^{II}$	0.0	(1)
$X^{II-} + K^+ \leftrightarrow KX^{II}$	2.1	(1)
$X^{II-} + Cs^+ \leftrightarrow CsX^{II}$	3.6	(1)
FES		
$X^{FES-} + Na^+ \leftrightarrow NaX^{FES}$	0.0	(1)
$X^{FES-} + K^+ \leftrightarrow KX^{FES}$	2.4	(1)
$X^{FES-} + Cs^+ \leftrightarrow CsX^{FES}$	7	(1)
$X^{FES-} + NH_4^+ \leftrightarrow NH_4X^{FES}$	3.5	(1)

(1) Bradbury and Baeyens (2000).

(2) Brouwer et al. (1983).

(a) Value assumed, considering equal sorption behaviour for Mg^{2+}, Ca^{2+} and Sr^{2+}.

Table 3-3. Calculated initial composition of the cation exchange sites.

Site	mol·L_{water}^{-1}
Planar sites	
CaX_2	1.19×10^{-3}
NaX	4.72×10^{-4}
MgX_2	3.29×10^{-4}
KX	7.54×10^{-5}
SrX_2	3.76×10^{-6}
CsX	1.08×10^{-9}
$^{LAB}SrX_2$	5.89×10^{-15}
Type II sites	
KX^{II}	5.53×10^{-4}
NaX^{II}	3.47×10^{-4}
CsX^{II}	7.89×10^{-8}
FES	
NH_4X^{FES}	4.96×10^{-6}
KX^{FES}	4.21×10^{-6}
NaX^{FES}	1.32×10^{-6}
CsX^{FES}	7.56×10^{-7}

3.5 Results

3.5.1 Comparison of results for non-reactive transport

In order to check the implementation of FASTREACT, a verification exercise has been carried out. This verification consists in comparing the average conservative breakthrough curves at CP2 computed using FASTREACT and the purely Lagrangian approach (i.e. the particle tracking simulations). Figure 3-7 shows the comparison of the breakthrough curves computed using the two approaches for realisation F4 (the remaining realisations are not shown here for the sake of brevity). All the concentrations thereafter are normalised by the average concentration at the left boundary (i.e. the injection boundary).

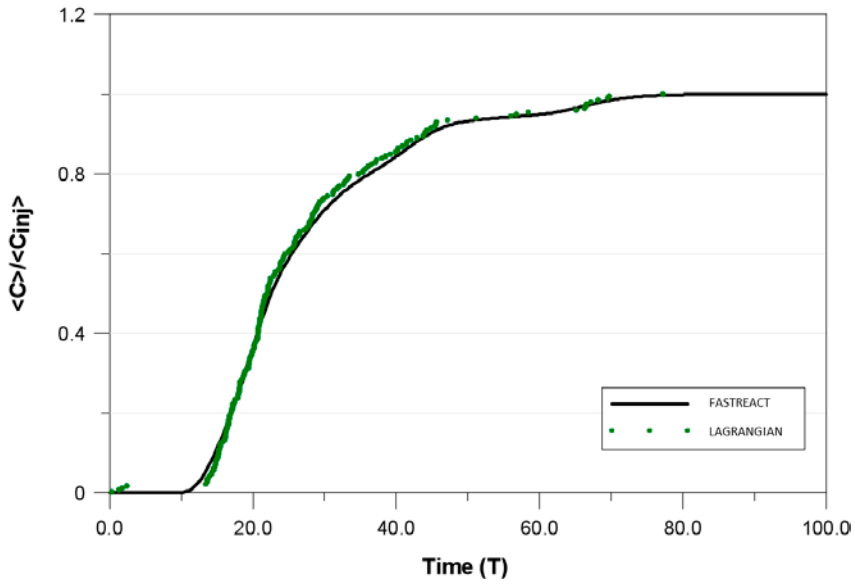

Figure 3-7. *Realisation F4: average breakthrough curve at control plane CP2 for a conservative solute computed using the Lagrangian approach (dots) and FASTREACT (continuous line).*

It can be noticed that FASTREACT tends to slightly smoothen the breakthrough curve. This is attributable to the discretisation of the reference simulation. In other words, if the discretisation is not fine enough, trajectories having similar travel times may pass through the same reference cell. Overall, the agreement between the two solutions is good meaning that the methodology has been properly implemented.

3.5.2 Comparison of results for reactive transport

As explained in the Introduction, one of the objectives of this work is to analyse the validity of FASTREACT when applied to synthetic heterogeneous media and get some qualitative insight into the implications of the underlying assumptions on the results. To this aim, the reactive transport problem illustrated in Section 3.2 has been solved using both the "standard" Eulerian approach (Section 3.3.1) and FASTREACT (Section 3.3.3) for the five selected realisations (Figure 3-4). The results provided by the two methodologies have then been compared and discussed.

It is worth noting that the Eulerian approach, as all mesh-based methods, has some difficulty in accurately simulating multidimensional advection-driven problems due to numerical dispersion that introduces artificial mixing and dilution of the plume (e.g. Zheng and Wang 1999, Herrera et al. 2009). Nonetheless, although numerical dispersion cannot be fully removed, it can be minimised using an accurate time and space discretisation.

If we consider an average velocity estimated from the geometric mean of the heterogeneous hydraulic conductivity fields (i.e. K_G=*1 L/T*) in our examples, which are solved using PHAST, the Peclet number (*Pe*) and the Courant number (*Co*) are within the ranges required to minimise numerical oscillations (Fletcher 1991):

$$Pe = \frac{\delta}{\alpha_L} = 2.0 \qquad Co = \frac{|v| \cdot \Delta t}{\delta} = 0.4 \qquad \text{3-11}$$

where δ is the grid size, α_L is the longitudinal dispersivity, v is groundwater velocity and Δt is the time step. The analysis of Figure 3-8 shows that the breakthrough curves computed by PHAST are not very sensitive to the grid Peclet number tested, indicating that the discretisation used in this modelling exercise does not introduce additional numerical dispersion. It is, however, worth noting that the tested range of Pe numbers is quite modest.

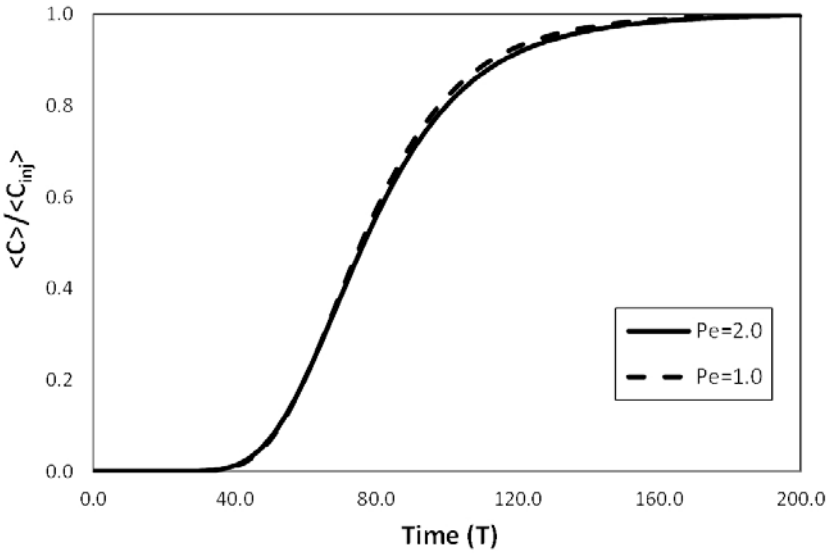

Figure 3-8. *Effect of the Peclet number on the PHAST results (realisation F1, average breakthrough curve at CP1).*

Figure 3-9 shows the distributions of particle travel times at CP1 for realisations F1 and F2. Although these fields are obtained from two realisations of the same random functions, it can be seen that their degrees of connectivity (as indicated by the concentration of flow paths to a small portion of the domain) are very different. In fact, from the histograms one can observe that the particles of F1 move fast and "homogeneously" indicating that channelling is a key outcome of this specific simulation.

Realisation F2 shows a different behaviour where the variability of travel times is high and their mean value indicates that the average velocity is lower. These different degrees of connectivity, which are linked to the small size of the domain compared to the correlation scale of *ln K* (see Section 3.2.2), can be related to the relative importance of the different transport processes (i.e. advection vs. local dispersion) and thus to the suitability of FASTREACT when applied to a given realisation.

Figure 3-10 shows the comparison of the average breakthrough curve at CP1 for the conservative solute and for the five considered realisations. It is worth noting that if compared with FASTREACT, the time of the first solute arrival computed by PHAST is smaller in all the realisations. This is probably attributable to the effects of numerical dispersion discussed above. The agreement between the two methodologies is good for all the considered cases.

Yet, one can observe that this agreement is best in those realisations having fast travel times (i.e. F1, F3 and F5), while those realisations characterised by a lower degree of connectivity show relatively poorer agreement. This may indeed be attributed to the effect of mixing, which is neglected in the FASTREACT approach. As explained before, the relative importance of transverse dispersion increases when the Peclet number of the problem decreases. It turns out that the effect of mixing becomes particularly relevant in those realisations with "slow advection".

The same comparison has been carried out for the reactive solute (i.e. the labelled strontium of Section 3.4, thereafter denoted as strontium). From the results (Figure 3-11), it can be seen that the degree of accuracy of FASTREACT is not substantially different from that observed for the conservative tracer. The "equivalent retardation factor" of the reactive tracer is approximately 1.8; this entity expresses the delay of the breakthrough curve for reactive transport relative to that for the conservative solute, implying that the results are interpreted in terms of a model for linear equilibrium sorption.

Figure 3-12 compares the average breakthrough curves of realisation F5 computed at the three different control planes: CP1, CP2 and CP3. Qualitatively, it is difficult to observe a pattern that relates the "goodness" of the agreement with the number of integral scales sampled by the plume. Nonetheless, a more rigorous analysis on the effect of the correlation length of the underlying conductivity field requires further investigations that are out of the scope of the present work.

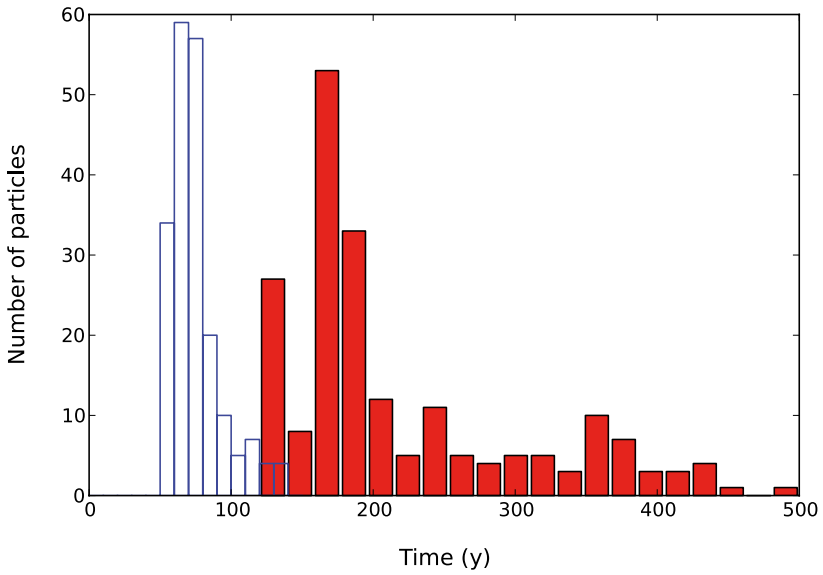

Figure 3-9. *Histogram showing the distribution of particle travel times at CP1 for realisations F1 and F2.*

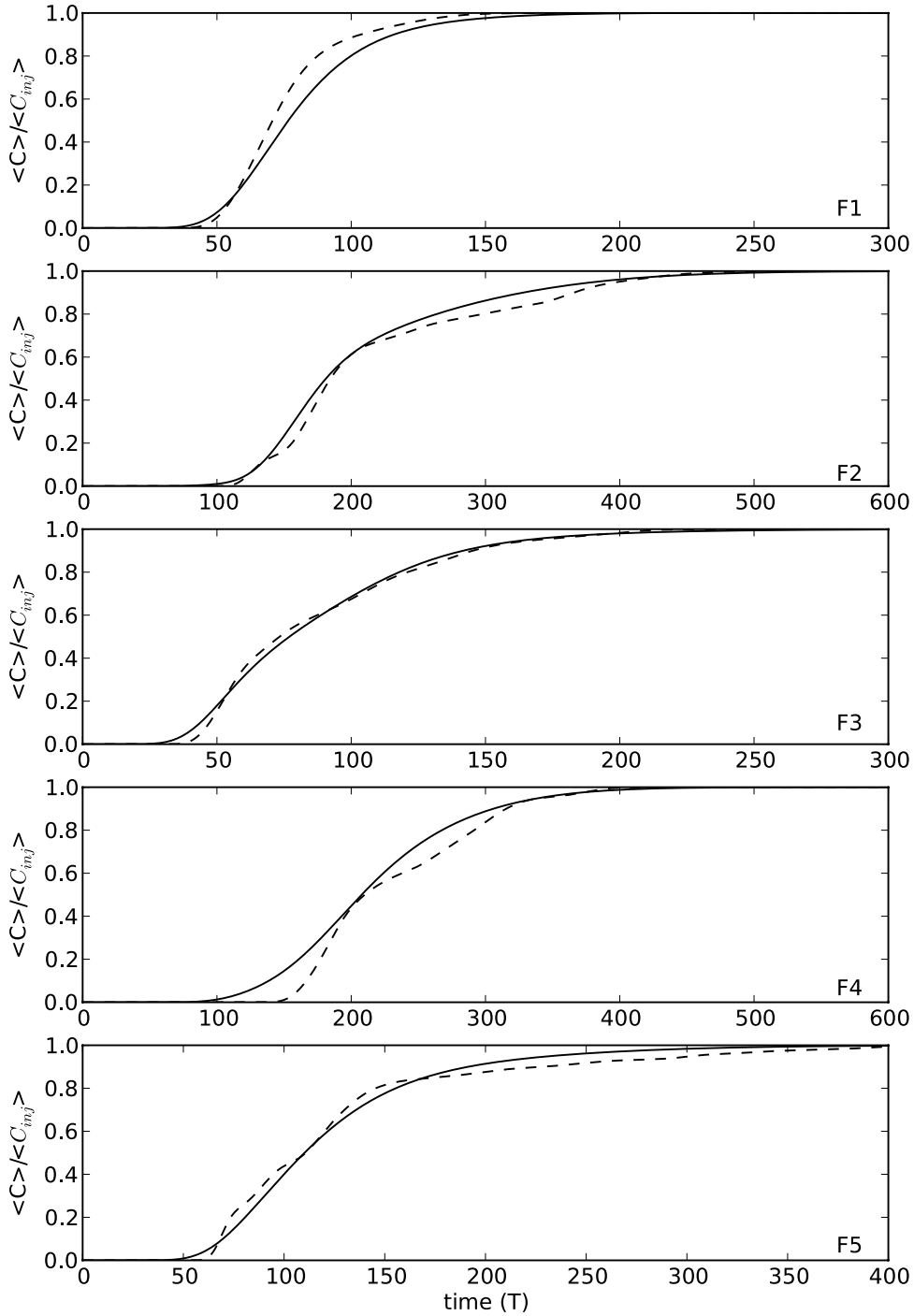

Figure 3-10. *Conservative solute – Normalised average breakthrough curves at CP1 computed with the Eulerian approach and FASTREACT (continuous line and dashed line, respectively).*

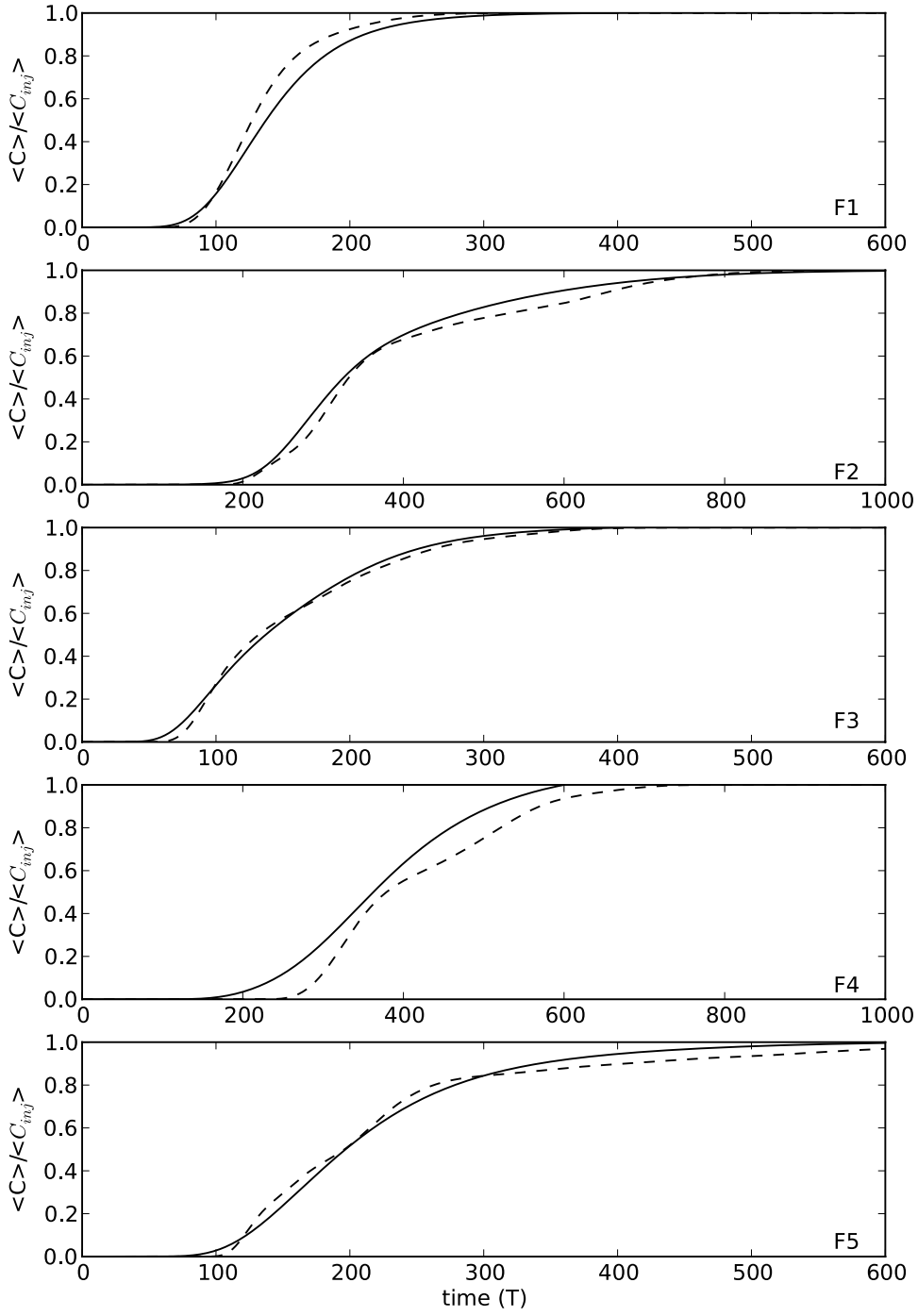

Figure 3-11. *Reactive solute (Sr) – Normalised average breakthrough curves at CP1 computed with the Eulerian approach and FASTREACT (continuous line and dashed line, respectively).*

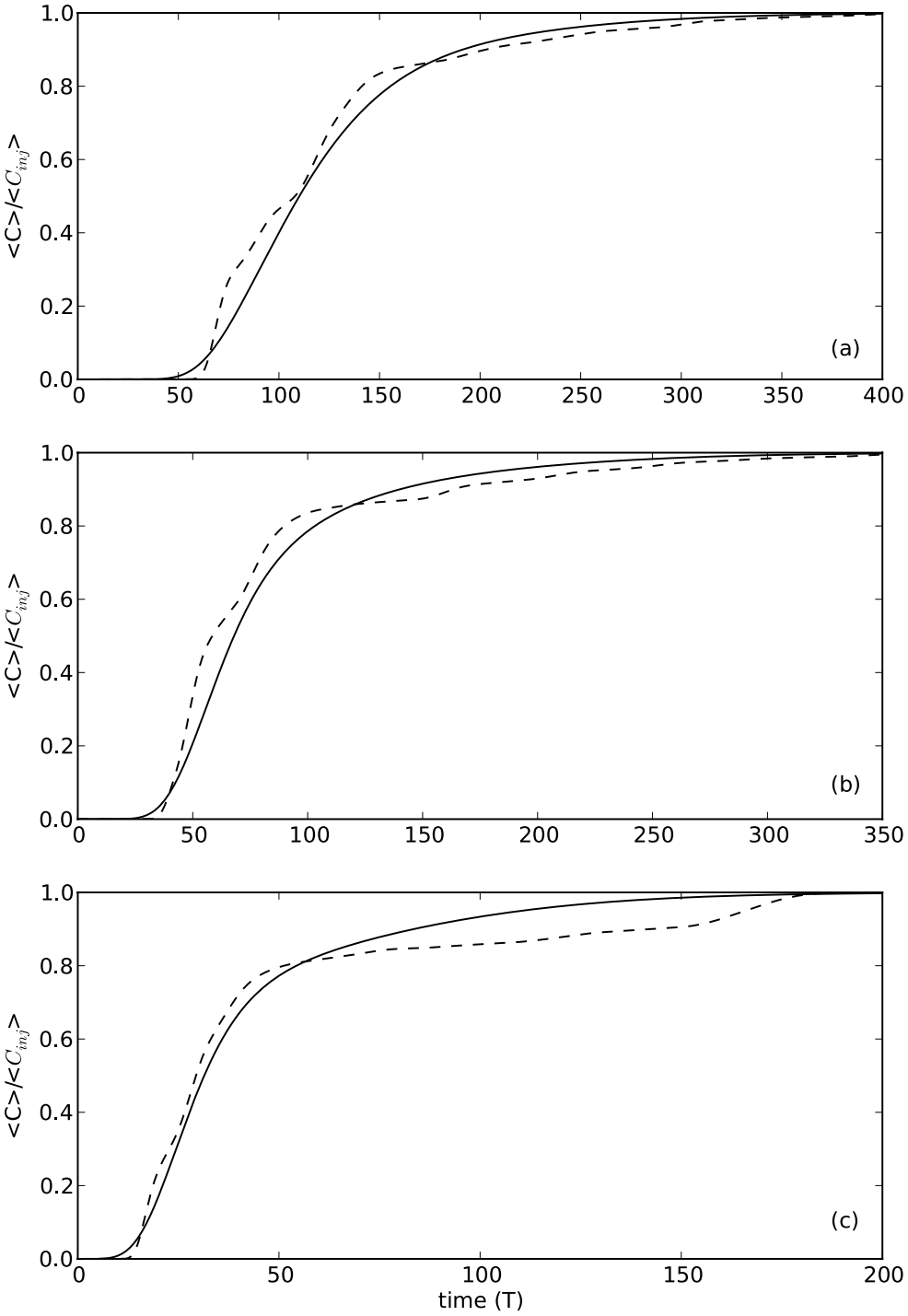

Figure 3-12. *Conservative solute – Normalised average breakthrough curves for realisation F1 computed at (a) CP1, (b) CP2 and (c) CP3 using the Eulerian approach and FASTREACT (continuous line and dashed line, respectively). See Figure 3-3 for the location of the control planes CP1, CP2 and CP 3.*

In summary, a comparison exercise has been carried out by solving a relatively simple reactive transport problem using both a "standard" Eulerian approach and FASTREACT. The simulations have been performed over a set of multi-Gaussian hydraulic conductivity fields. It is worth noting that multi-Gaussian models are not particularly suitable for FASTREACT since they rely on a maximisation of the field entropy (i.e. spatial disorder), which minimises flow and transport channelling (Gómez-Hernández and Wen 1998) thus magnifying the importance of transverse dispersion.

Even so, the results show a good agreement for all the considered heterogeneous fields. This agreement seems to be inversely related to the Peclet number of the problem, which means that it is best in the simulations that are "advection-dominated" (F1, F3 and F5), and somewhat poorer in the realisations with "low velocities" (F2 and F4). No significant differences in the resulting agreement are observed for the reactive species.

3.6 CPU performance

As discussed above, the key point of stochastic-convective models is that they allow representing reactive transport processes taking place in complex two- or three-dimensional systems by a set of independent one-dimensional problems. Furthermore, the FASTREACT methodology borrows from the LaSAR-PHREEQC approach presented by Malmström et al. (2004, 2008) the idea of mapping the entire set of streamline using one single PHREEQC simulation. It turns out that the main advantage of the FASTREACT approach compared to "standard" Eulerian simulations lies in its outstanding computational efficiency. Here, we try to quantify this efficiency by comparing the execution times required by the Eulerian and FASTREACT approaches when simulating each of the considered realisations.

The simulations were carried out on a Windows XP desktop computer with an Intel Core 2 Quad processor (2.4 GHz, 2 GB RAM). Table 3-4 summarises the time of calculation taken by each simulation and each methodology. For what concerns FASTREACT, the time taken by the particle tracking runs is negligible if compared with the time taken by the PHREEQC simulations.

The execution time of the Eulerian simulation depends largely on the average plume velocity since it conditions the simulation time needed to obtain a representative breakthrough curve at the considered control plane. For instance, from Figure 3-11 one can see that in a highly connected field (e.g. F1) the breakthrough curve of the reactive solute reaches the plateau after 300 time units while in a poorly connected field (e.g F2) the elapsed time can extend up to 1,000 time units. This is reflected in the execution times of the two simulations: 230 minutes for F1, 769 minutes for F5.

Table 3-4. Execution time (minutes) of each realisation for the two numerical approaches.

Realisation	Eulerian approach	FASTREACT approach
F1	230'	33'
F2	769'	50'
F3	308'	33'
F4	615'	50'
F5	400'	33'

As explained before, the execution time of FASTREACT depends on the distribution of travel times of the considered simulation at the considered control plane. For instance, if one looks at the particle travel times of realisation F1 and F2 (Figure 3-9), one can see that the former is characterised by a narrow distribution while the latter has a great variability with travel times spanning a very wide range. It turns out that realisation F1 needs a relatively 'short' PHREEQC reference simulation to cover the entire set of travel times while realisation F2 is linked to a considerably "larger" reference simulation. This is directly reflected in their related execution times: 33 minutes for F1, 50 minutes for F2.

Overall, we can say that the execution time of FASTREACT is approximately one order of magnitude lower than that taken by the Eulerian approach. It should be stressed that this modelling exercise relies on a relatively simple two dimensional domain discretised into a few thousand elements. In a more complex three dimensional system, the difference between the execution times of the two approaches is expected to increase dramatically thus increasing the advantages provided by FASTREACT in terms of efficiency.

4 Application example

4.1 Introduction

In this section we show a real-case application where the adoption of the FASTREACT approximation allows large-scale reactive transport simulations to be performed by coupling sets of 1D reactive transport simulations to ensembles of streamlines computed over a complex three-dimensional hydrogeological model (consisting of more than 5 million elements). The modelling work and the results presented here are part of a project focused on the prediction of the hydrogeochemical evolution at the Olkiluoto site (Finland) in the context of the Posiva safety case. Here, we present a summary of the methodology and some example results obtained for the post-operational period (from now on denoted as temperate period). For a detailed account of the modelling approach and the results computed for the different simulation periods (spanning one glacial cycle) the reader is referred to Trinchero et al. (2014).

4.2 General idea

The main idea behind this work is that the hydrochemical evolution in the rock surrounding the repository is the result of infiltration processes that occur from the surface of the domain. The infiltrating groundwater undergoes chemical changes as a result of different water-rock interaction processes (e.g. mineral dissolution and precipitation, surface complexation, and cation exchange). Furthermore, in a fractured medium such as the bedrock at Olkiluoto, groundwater is usually channelled through an extensive and complex network of fractures and deformation zones. Thus, it is reasonable to assume that different parts of the repository are affected by different recharge paths, which in turn can be treated independently.

The first step of the modelling exercise consists in defining a control plane (or a number of control planes), which includes the whole repository. The control plane is subdivided into 3,910 geometrically based cells, each of them being representative of parts of the plane affected by single specific recharge paths. These paths are then delineated using particle-tracking simulations; one particle is injected in the centre of each cell and backtracked to the surface (Figure 4-1 – see also Figure 2-3). Finally, the concentration in each cell in the control plane is provided by that grid cell of the related reference simulation whose travel time is equal to the travel time of the considered infiltration path (see Figure 4-2).

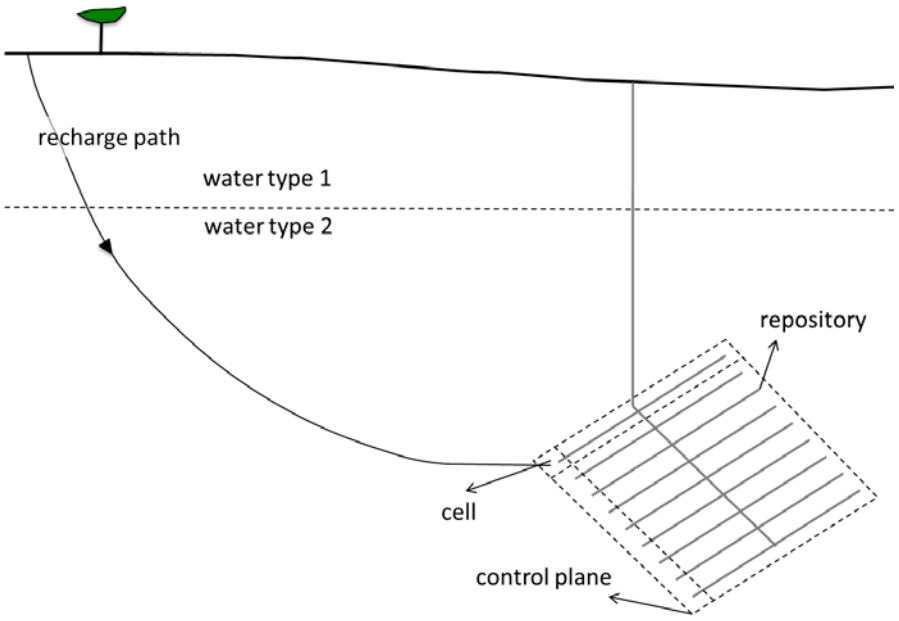

Figure 4-1. *Illustrative sketch of the modelling approach.*

4.3 Homogenisation procedure

As specified in Section 2, the FASTREACT methodology is suited for systems where the initial conditions are homogeneous (i.e. same mineral distribution and initial water throughout the whole domain). Nevertheless, in the case of Olkiluoto, we have to deal with a geological medium where groundwater is chemically stratified (see Figure 4-1 and Section 4.5.1). Thus, to account for these heterogeneous initial conditions (i.e. different groundwater types initially present at different depths), we have defined and used an approximation referred to as a "homogenisation procedure".

The procedure is illustrated in Figure 4-2. If we consider two path lines, path A and B, along which it takes t_i^A and t_i^B, respectively, to travel from the surface to the water interface ($t_i^A \neq t_i^B$), the homogenisation procedure consists in assuming that both path lines cross the interface at the same time. An equivalent time, t_e, is thus used to describe the travel time to this interface; t_e is defined based on expert judgment. The related reference simulation is then subdivided into two zones, having different initial water compositions. In this reference simulation the interface between the two zones is placed at node n, where n is given by:

$$n = \mathrm{int}\left(\frac{t_e \cdot v}{\Delta x}\right) + 1 \qquad 4\text{-}1$$

with v being the velocity and Δx the discretisation in the reference simulation (see Section 3.3.3).

In order to minimise the influence of this simplifying assumption, fairly homogeneous groups of recharge paths have to be defined. This is done based on expert judgment and prior to the modelling process. A single one-dimensional reactive transport simulation is then used to describe each group of paths.

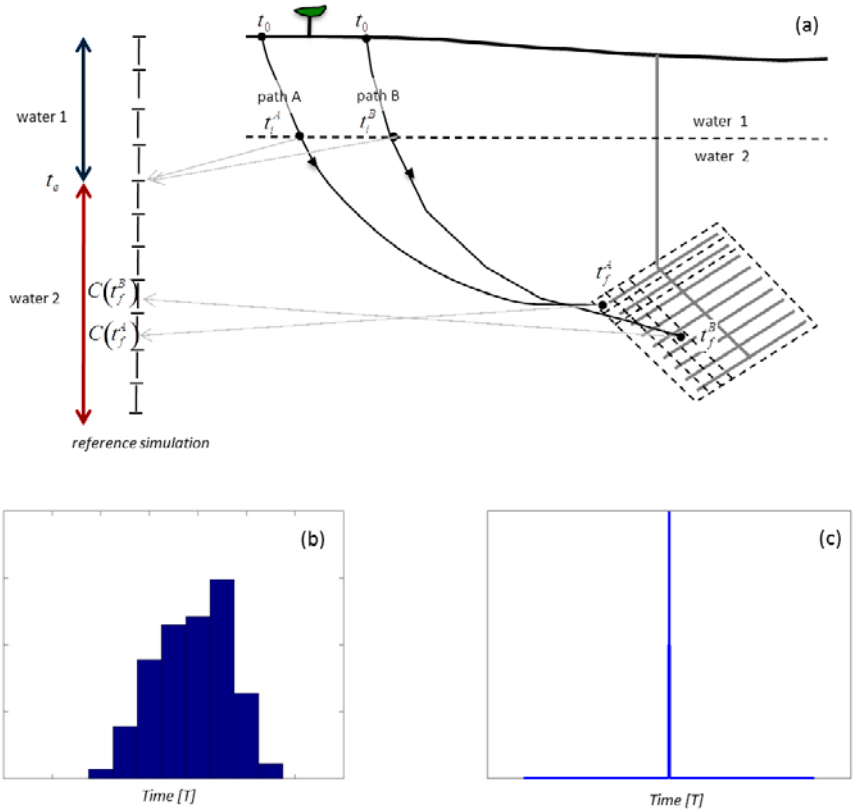

Figure 4-2. *(a) Illustrative sketch of the homogenisation procedure. When dealing with many streamlines, the homogenisation procedure consists in describing (b) the travel time histogram to the ith interface using (c) a Dirac delta function $\delta(t-t_e)$ where t_e is the equivalent travel time.*

4.4 Methodology

The hydrogeochemical changes and evolution at repository depth are strongly conditioned by the hydrogeological conditions of the site, which in turn depend on the specific operational stages in the repository as well as on the changes caused by variations in the climatic conditions. Thus, in the definition and implementation of these reactive transport simulations, strong emphasis has been placed on the need for integrating information coming from existing hydrogeological regional models. This has been achieved following a stepwise methodology that can be summarised as follows:

1. The simulation time frame, spanning one glacial cycle, is divided into sub-periods according to the conditions of the repository (open repository or closed repository) and the climatic conditions at the surface (temperate period or melting period). In this report, only the results of the post-operational temperate period with a closed repository are presented.
2. For each considered period (operational, temperate and glacial – see Figure 4-3) in the analysis of the whole glacial cycle (of which only the temperate part discussed in detail here), a snapshot of the velocity field is taken from the hydrogeological model of Löfman et al. (2009), see Figure 4-4. The velocity field is assumed to be constant during the simulated period.
3. For each considered period and using the velocity field identified in step 2, 3,910 particles are injected at repository depth (see Figure 4-5) and backtracked to the surface. The simulations, which are performed using the random walk particle tracking code RW3D-MT (Fernàndez-Garcia et al. 2005), aim at delineating the infiltration paths and calculating corresponding travel times.
4. In order to minimise the effect of the homogenisation procedure used to define initial conditions (see Section 4.5.1), the particle trajectories are grouped according to their travel time and geometry. Each group of particles is then used to parameterise the corresponding PHREEQC reactive transport simulation.
5. The total travel time of a given trajectory (i.e. particle) is used to relate the considered cell of the control plane to the corresponding reference cell of the PHREEQC simulation (see Figure 4-2). This allows producing maps of concentration at repository depth and at different simulation times (note that no interpolation is done from one cell to the other).

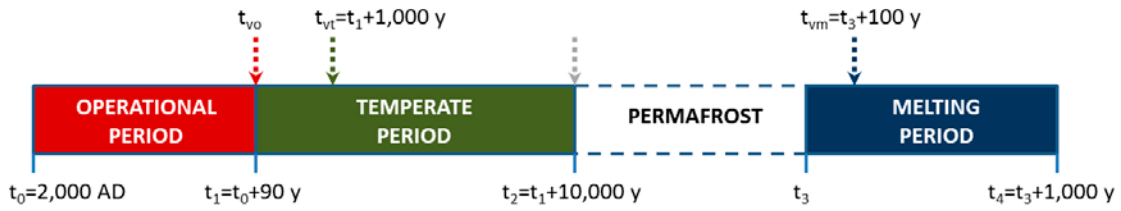

Figure 4-3. *Sketch of the sequence of operational and climatic periods modelled in the framework of the POSIVA safety case (figure taken from Trinchero et al. 2014). In the present work only the results of the temperate period are shown. The arrows indicate the time at which each snapshot of the velocity field has been taken.*

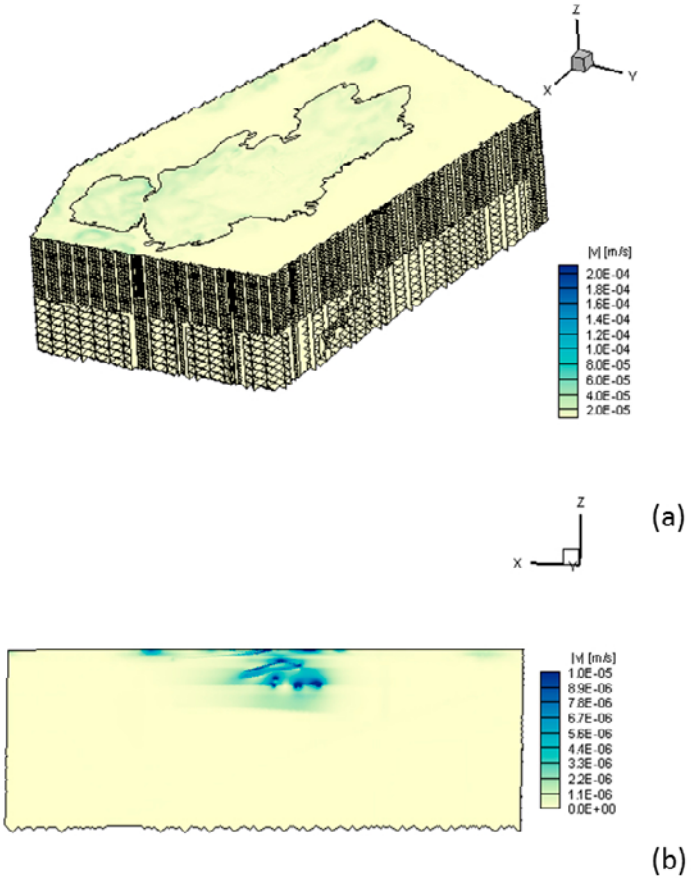

Figure 4-4. *Magnitude of the groundwater velocity vector at $t=t_{vt}$ (results taken from the model of Löfman et al. 2009) (a) over the whole model domain and (b) along the vertical cross-section shown in Figure 4-6 (figure taken from Trinchero et al. 2014).*

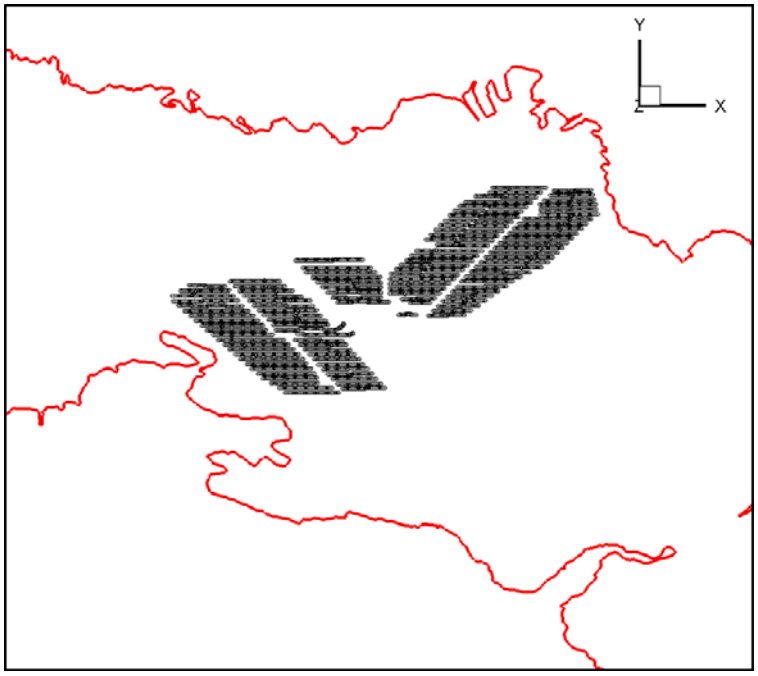

Figure 4-5. *Plan view of the initial location of the 3,910 particles injected at repository depth and backtracked to the surface (figure taken from Trinchero et al. 2014).*

4.5 Model set-up

4.5.1 Initial conditions

The groundwater at Olkiluoto is stratified according to different physicochemical factors (Posiva 2009). Generally, the salinity of the water increases with depth (Figure 4-6). This water stratification has direct implications on the model implementation and parameterisation. According to the existing prior information (Pitkänen et al. 2008) and the analysis of the available groundwater samples, three different hydrochemical zones have been defined where the initial groundwater chemical composition can be assumed homogeneous and be described by a single representative sample. The initial zonation of waters for the temperate simulation, which has been defined based on the results of the hydrogeological model (Löfman et al. 2009), is specified in Table 4-1. The same initial water is used for both the fracture and the matrix.

Table 4-1. Initial conditions of the reactive transport simulations; the table shows the elevations in metres above sea level of the interfaces between the different water types.

Interface	Elevation
Brackish HCO3/Brackish SO4 (S1/S2)	–120.0
Brackish SO4/Brackish saline (S2/S3)	–380.0

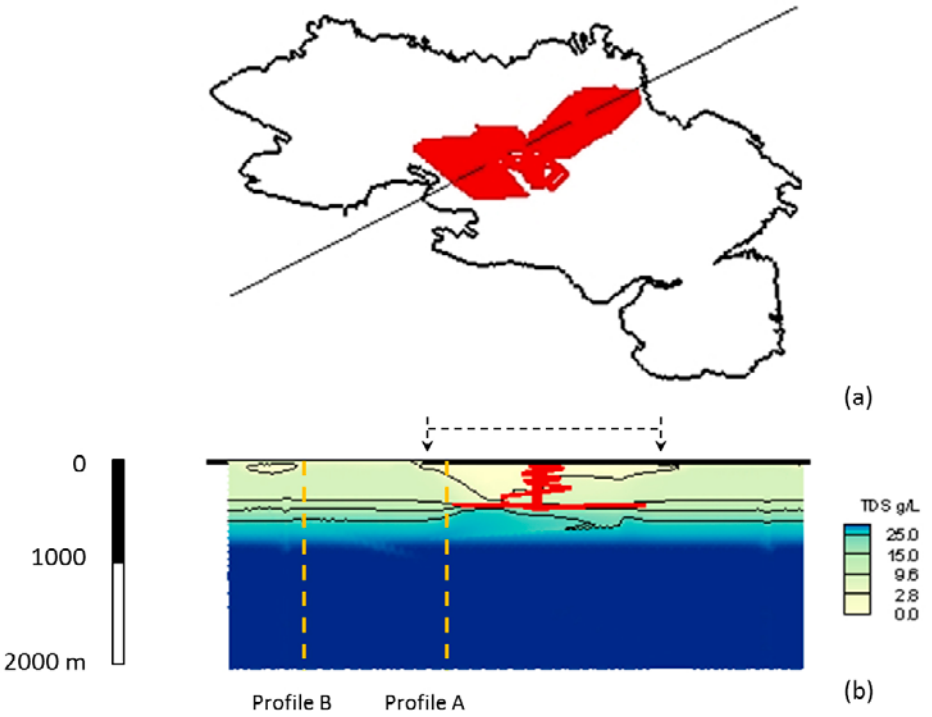

Figure 4-6. *TDS values computed by the hydrogeological model (Löfman et al. 2010) at the end of the operational period: (a) cross-section and (b) vertical profile (yellow dashed lines) used for the definition of the initial hydrochemical zones (figure taken from Trinchero et al. 2014).*

4.5.2 Random walk particle tracking simulations

The selected modelling period spans an entire temperate period (i.e. 10,000 years) considering as "starting point" the closure of the repository. The ensemble of streamlines is obtained using a snapshot of the velocity field taken at $t=t_{vt}$ (i.e. after 1,000 years from the beginning of the hydrogeological simulation – see Figure 4-3). All particles move along relatively straight pathlines from the centre of the island above and down to the repository (Figure 4-7). This homogeneity is further confirmed by the travel time histogram (Figure 4-8), which shows a mono-modal distribution resembling a Gaussian function with mean and standard deviation equal to 225 years and 37 years, respectively.

To reduce the implications of the simplifying assumption used to define the model initial conditions (see Section 4.3), the ensemble of trajectories are grouped according to their travel times. As explained in the above-mentioned section, these subgroups and the related equivalent travel times to the different interfaces are based on expert judgement. The groups of trajectories are summarised in terms of travel times in Table 4-2, and the trajectories are illustrated in Figure 4-9. The travel time statistics of each group of trajectories are analysed in order to parameterise the related PHREEQC simulations. The histograms of the total travel time and the time of travel to the different interfaces as well as the equivalent times used for model parameterisation are summarised in Figure 4-10 to Figure 4-12.

Table 4-2. Groups of trajectories and corresponding travel times.

Group	Travel time (years)
G1	130–158
G2	158–181
G3	181–206
G4	206–301

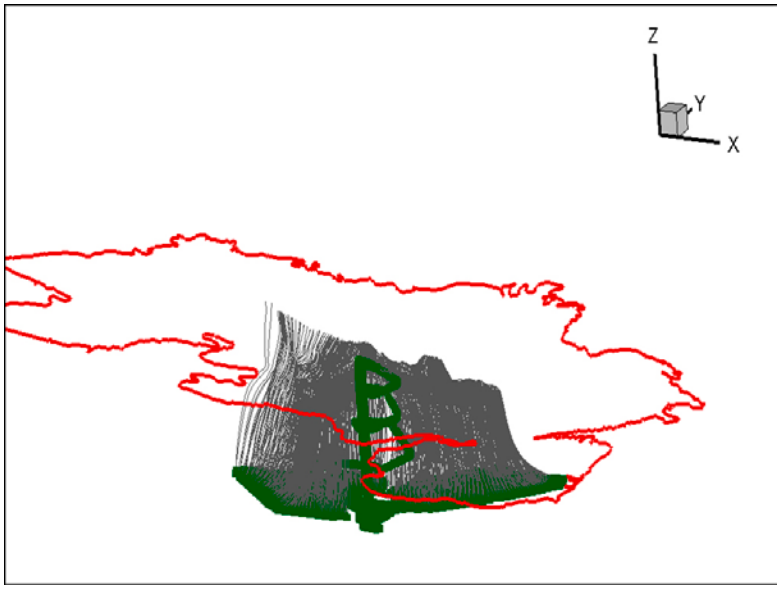

Figure 4-7. *Ensemble of particle trajectories (i.e. recharge paths from the surface to different parts of the repository) for the temperate period simulation (vertical exaggeration 1:2; figure taken from Trinchero et al. 2014).*

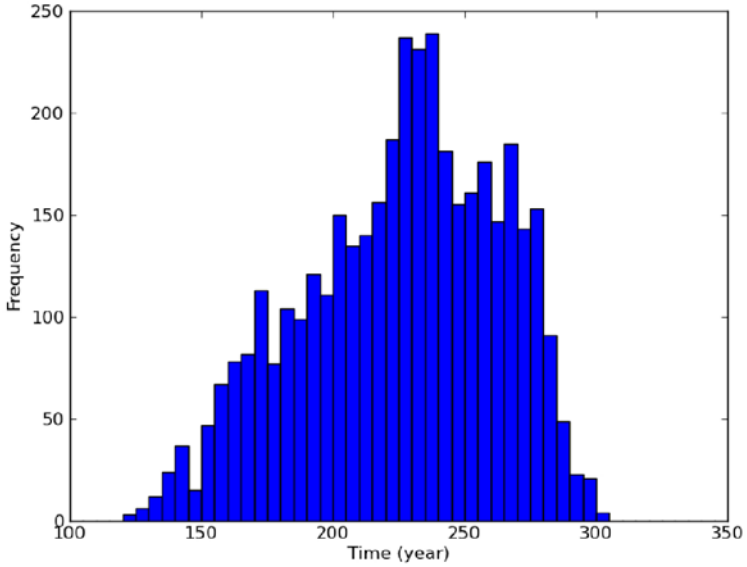

Figure 4-8. *Travel time histogram (i.e. distribution of travel times from the surface to the repository) for the ensemble of particles of the temperate period simulation (figure taken from Trinchero et al. 2014).*

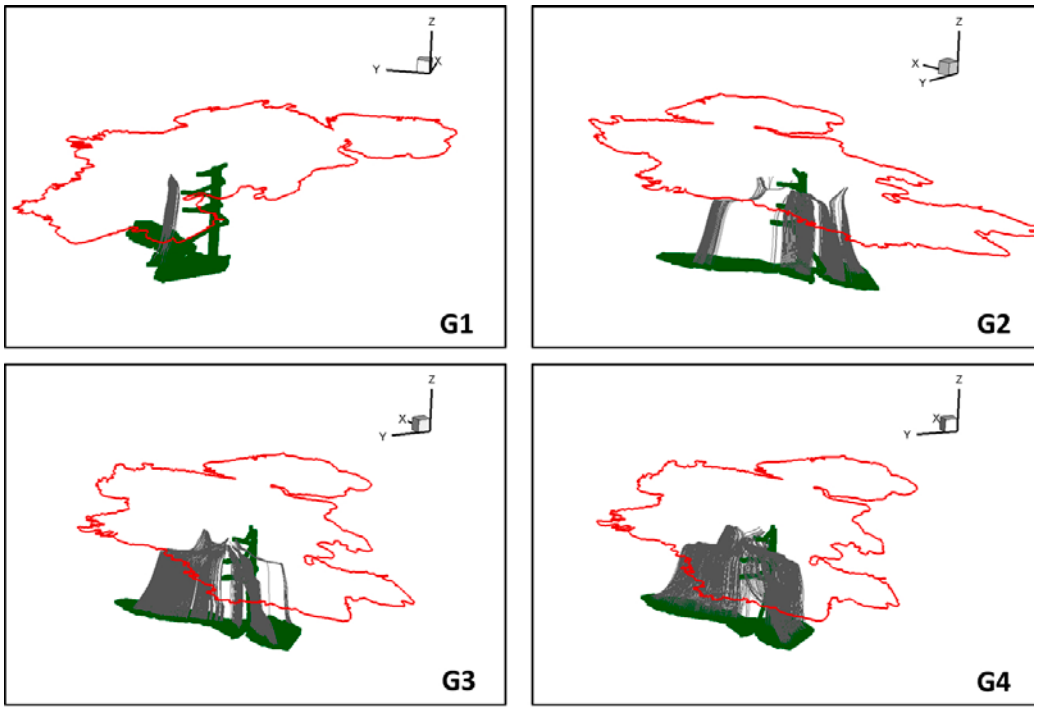

Figure 4-9. *Particle trajectories for the different groups specified in Table 4-2 (figure taken from Trinchero et al. 2014).*

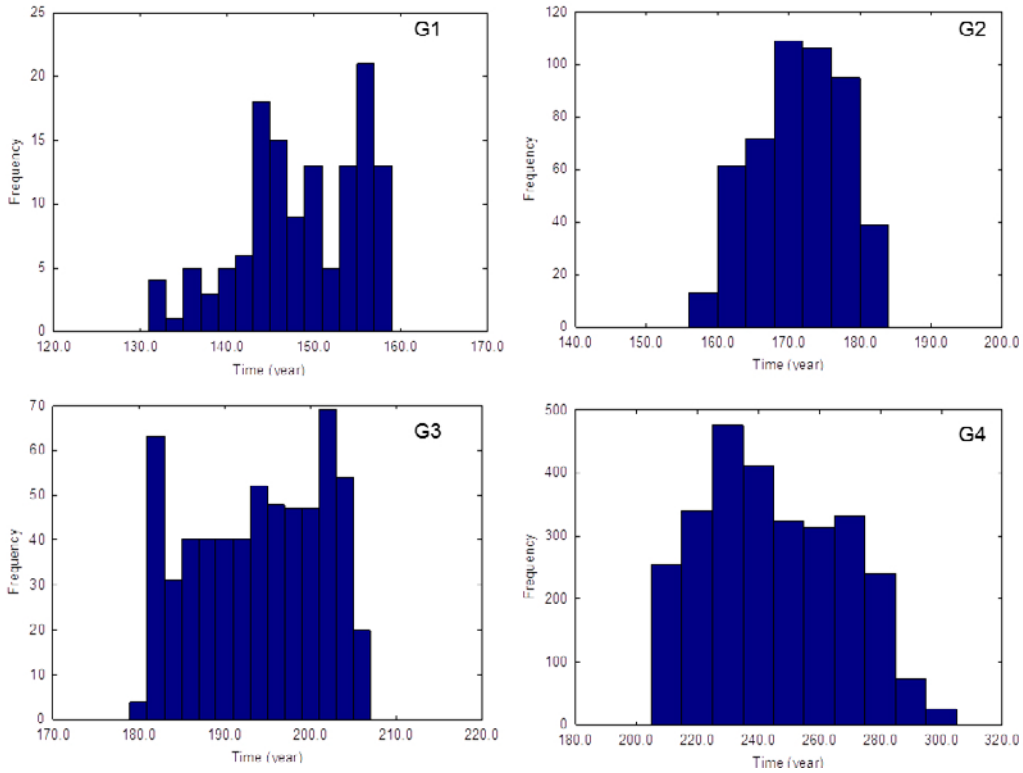

Figure 4-10. *Travel time histogram for each group of particles of the temperate period simulation (figure taken from Trinchero et al. 2014).*

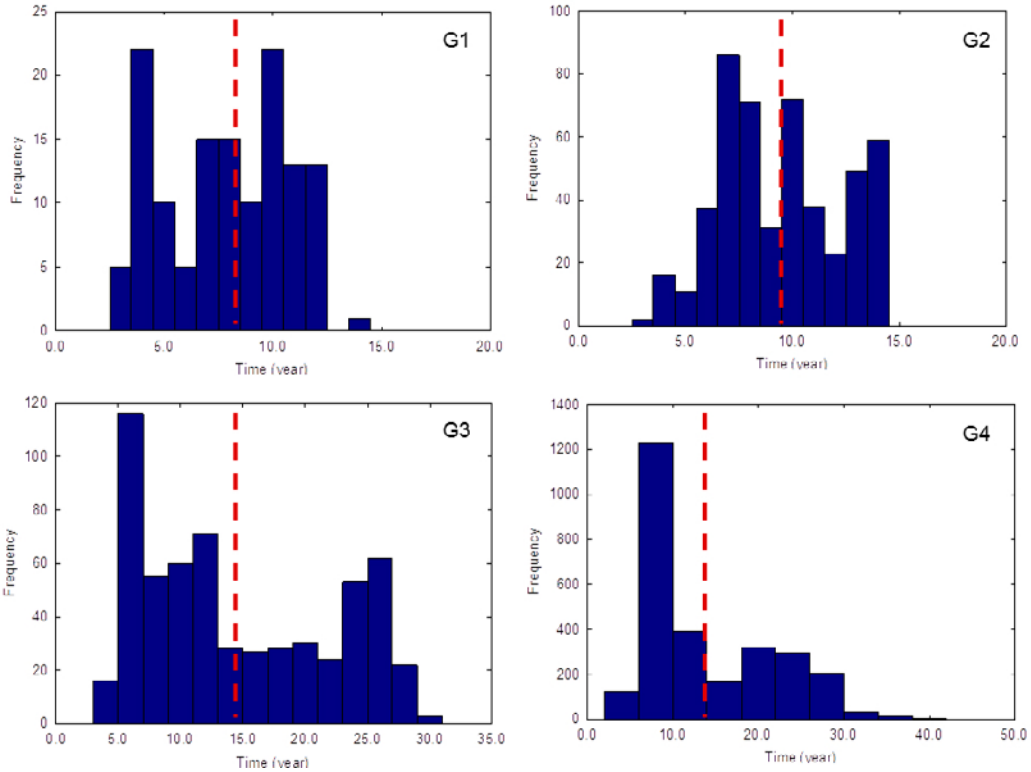

Figure 4-11. *Travel time from the surface to the interface S1/S2 (Table 4-1) for each group of particles of the temperate period simulation. The dashed line indicates the equivalent time (t_e) used in the homogenisation procedure (figure taken from Trinchero et al. 2014).*

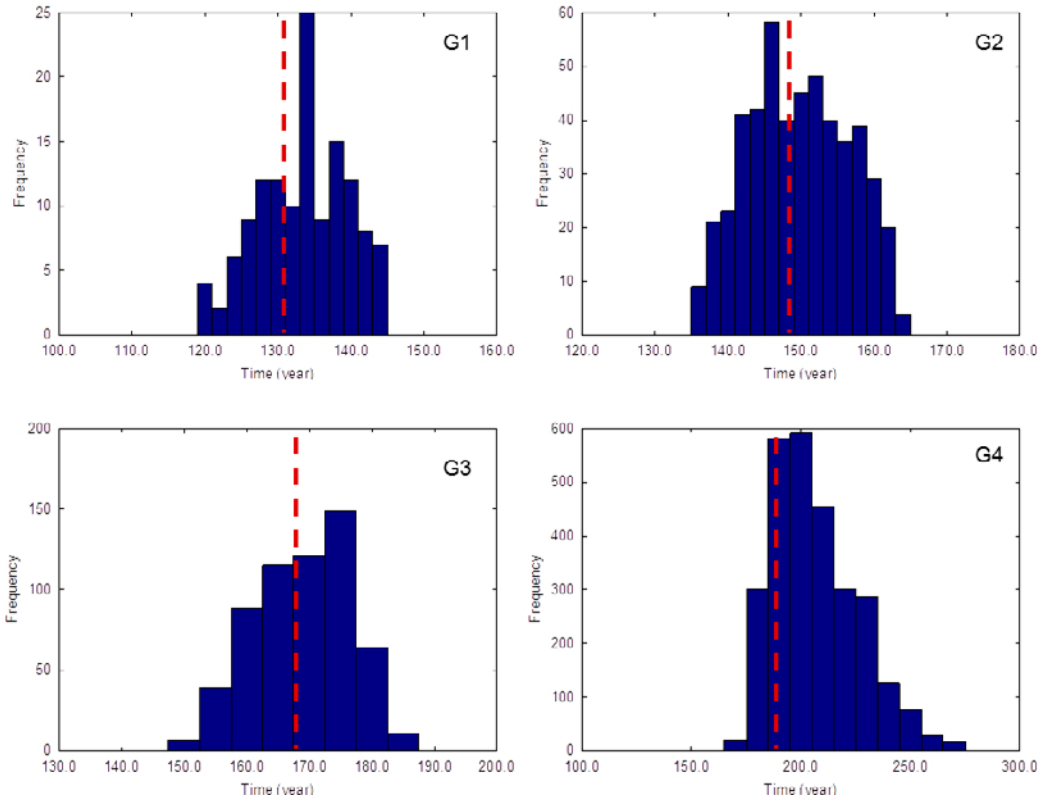

Figure 4-12. *Travel time from the surface to the interface S2/S3 (Table 4-1) for each group of particles of the temperate period simulation. The dashed line indicates the equivalent time (t_e) used in the homogenisation procedure (figure taken from Trinchero et al. 2014).*

4.5.3 Dual porosity formulation

To mimic the interplay between the "mobile" domain (i.e. deformation zones and fractures with relatively high hydraulic conductivity) and the low-conductive surrounding rock, a standard dual-porosity approach has been adopted. The dual porosity representation of the fractured medium is analogous to that used by Löfman et al. (2009) where the two continua (i.e. matrix and fractures) are described by a parallel fracture model (Figure 4-13).

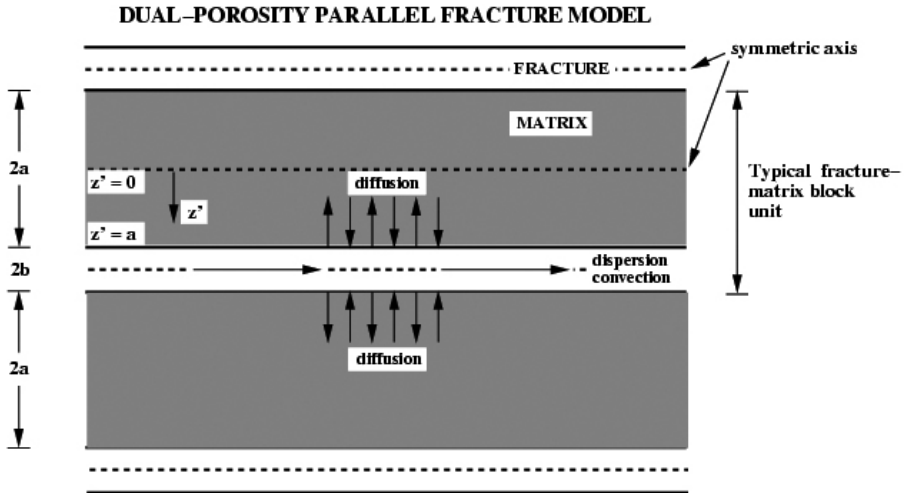

Figure 4-13. *Parallel fracture model used to described the fractured system (modified from Löfman et al. 2009).*

For each aqueous component, the general form of the reactive transport equation in the mobile part of the system can be written as follows:

$$\frac{\partial c_m^j}{\partial t} = \nabla \cdot \frac{D}{\phi_m} \nabla c_m^j - \nabla \cdot v c_m^j - \Gamma + f \qquad 4\text{-}2$$

where c_m^j is the total aqueous concentration of component *j* in the mobile domain [mol L^{-1}], ϕ_m is the porosity of the mobile domain [–], ***D*** is the dispersion-coefficient tensor [m^2 s^{-1}], *f* is a source/sink term that accounts for kinetic and equilibrium reactions as well as sources or sinks of water [mol L^{-1} s^{-1}] and Γ is an exchange term that accounts for mass transfer between the mobile (subscript *m*) and the immobile domain (subscript *im*) [mol L^{-1} s^{-1}]:

$$\Gamma = \frac{1-\phi_m}{\phi_m} \frac{\partial c_{im}^j}{\partial t}\bigg|_{z'=a} \qquad 4\text{-}3$$

Since the immobile domain is dominated by diffusion, its governing equation is typically represented using Fick's law:

$$\frac{\partial c_{im}^j}{\partial t} = D_e \frac{\partial^2 c_{im}^j}{\partial z'^2} \qquad 4\text{-}4$$

where D_e the matrix effective diffusion coefficient [m^2 s^{-1}]. According to the Archie's law (Valkiainen 1992), the effective diffusion coefficient can be expressed as:

$$D_e = D_0 \cdot 0.71 \cdot \phi_{im}^{1.58} \qquad 4\text{-}5$$

where D_0 is the molecular diffusion in water [m^2 s^{-1}] and ϕ_{im} is the matrix porosity.

Equation 4-4 can be explicitly solved in PHREEQC using finite differences. Yet, this numerical scheme requires a tight control on model time step and grid spacing to minimise numerical dispersion (Lipson et al. 2007). This could not be guaranteed in our simulations because of their very large temporal and spatial scale. Thus, an alternative approach has been adopted in which the temporal derivative of Equation 4-4 is represented using a first-order exchange approximation (van Genuchten and Nielsen 1985):

$$\frac{\partial c_{im}^j}{\partial t}\bigg|_{z'=a} = \alpha \left(c_m^j - \overline{C}_{im}^j \right) \qquad 4\text{-}6$$

Here, $\overline{C}_{im}^j$ is the average concentration in the immobile zone [mol L^{-1}] and α is an empirical rate coefficient [s^{-1}] that can be expressed as (van Genuchten and Nielsen 1985):

$$\alpha = \frac{D_e}{\left(f_s \cdot \omega\right)^2} \qquad 4\text{-}7$$

where f_s is a shape factor [–] and ω is the characteristic length of the matrix [m]. In the case of a parallel fracture model, such as that illustrated in Figure 4-13, f_s and ω are 0.533 and *a* (i.e. half of the matrix thickness between fractures), respectively (van Genuchten and Nielsen 1985), while the mobile porosity is given by:

$$\phi_m = \frac{b}{b+a} \qquad 4\text{-}8$$

with *b* being half of the fracture aperture.

The values used for model parameterisation are summarised in Table 4-3. The initial groundwater composition of the matrix is assumed to be the same as that of the mobile domain (Table 4-1).

Table 4-3. Parameters and values used for the DP model parameterisation.

Symbol	Parameter	Value
a	Half matrix thickness	4.15 m[(1)]
b	Half fracture aperture	$1.83 \cdot 10^{-4}$ m [(1)]
D_0	Molecular diffusion coefficient in the water	$1.0 \cdot 10^{-9}$ m^2 s^{-1} [(2)]
ϕ_{im}	Matrix porosity	$1.0 \cdot 10^{-2}$ (–)[(2)]

[(1)] Table 4-2 Löfman et al. (2009). Arithmetic mean over the depth interval 0–400 m.
[(2)] Table 4-3 Löfman et al. (2009).

4.5.4 Geochemical conceptual model

The geochemical processes and the related model parameterisation rely on previous site characterisation studies of the Olkiluoto site (e.g. Posiva 2009). The key geochemical processes identified and implemented in the model are calcite and pyrite dissolution/precipitation, aluminosilicates weathering, cation exchange reactions, and aqueous redox reactions (Posiva 2009). Mineral dissolution and/or precipitation are simulated under equilibrium and/or kinetic assumptions depending on the mineral phase. The reader is referred to Trinchero et al. (2014) for a more detailed discussion of these processes as well as the numerical formalisms adopted to represent them in the numerical model.

4.6 Results

In this section, we present, in a summarised form, some of the results of the hydrochemical evolution modelling of the temperate period at the Olkiluoto site. It is worth stressing that the aim of this is not to provide a detailed discussion of the results of the hydrochemical evolution, but rather to highlight the potential of the methodology when applied to these types of problems.

The distribution of TDS, pH and Eh at repository depth and at different simulation times is shown in Figure 4-14, Figure 4-15, and Figure 4-16, respectively. One interesting evidence, stemming from these results, is the capability of the approach to capture the mutual interplay of different processes: advection through the mobile zone, geochemical reactions (e.g. the control of pH by calcite dissolution/precipitation, the control of Eh by the redox pair $FeS_2/Fe(OH)_3$) and the buffering effect of the rock matrix.

The role of the matrix is particularly evident if one looks at the TDS distribution (Figure 4-14). The "dilution" of the water in the repository, which is a consequence of the infiltration of "altered" meteoric water at the surface of the island, is very slow if compared with the particle travel times (Figure 4-8). This is explained by a continuous mass exchange that occurs between the mobile and the immobile domain (the same initial water composition is used for both the fracture and the matrix).

The analysis of the pH distribution highlights the effect of the heterogeneous initial conditions on the results. In fact, after 5,000 years part of the domain is affected by a slight increase in pH. This effect is explained by the signature of the brackish SO_4 water. After 10,000 years, part of this signature has been "removed" by the arrival of more diluted (and slightly more acidic) water. The evolution of the Eh distribution (Figure 4-16) results from the mutual effect of the arrival of different waters having slightly different redox conditions and the mineral control of the $FeS_2/Fe(OH)_3$ redox pair.

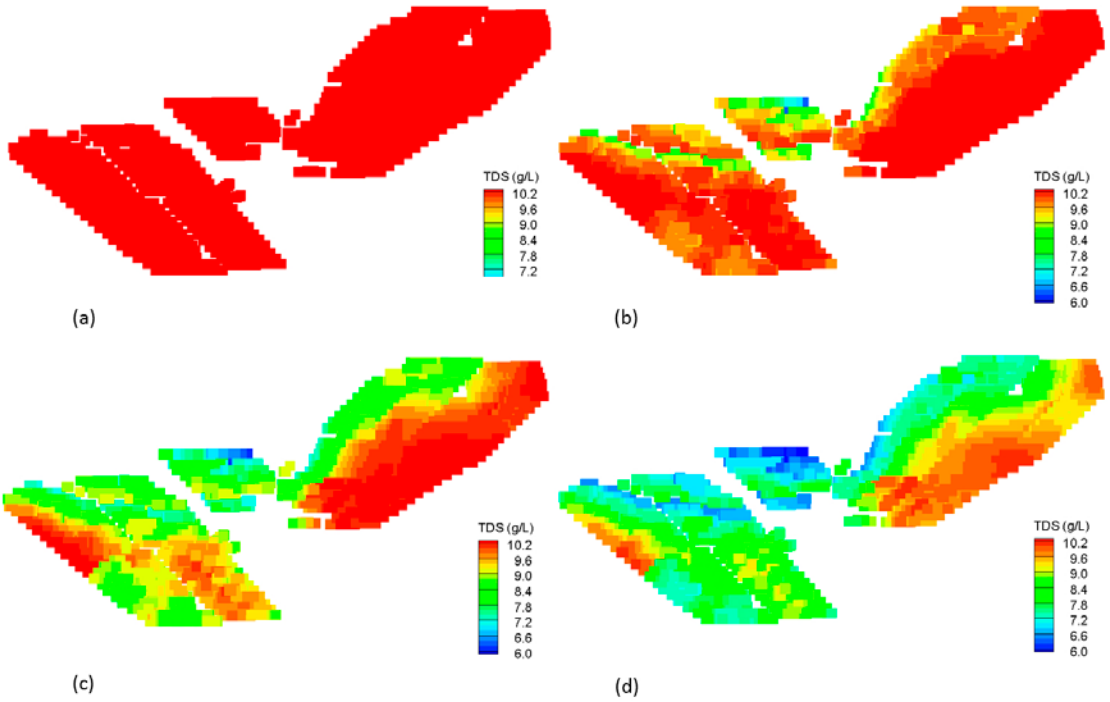

Figure 4-14. *Distribution of TDS at repository depth (a) at the beginning of the simulation, (b) after 1,000 y, (c) after 5,000 y and (d) after 10,000 y (figure taken from Trinchero et al. 2014).*

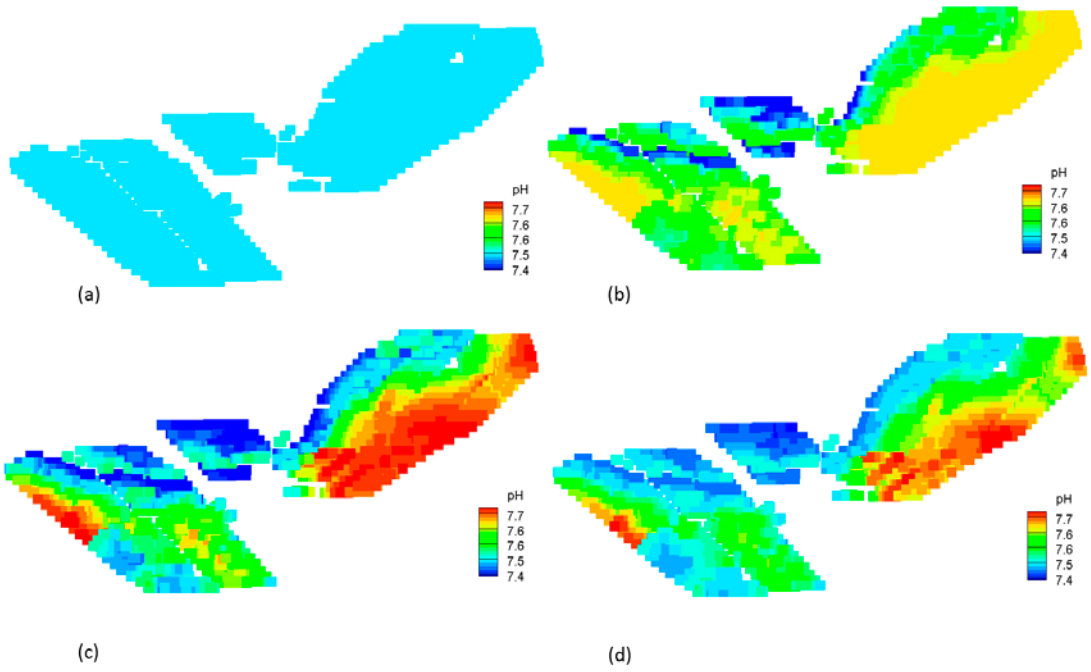

Figure 4-15. *Distribution of pH at repository depth (a) at the beginning of the simulation, (b) after 1,000 y, (c) after 5,000 y and (d) after 10,000 y (figure taken from Trinchero et al. 2014).*

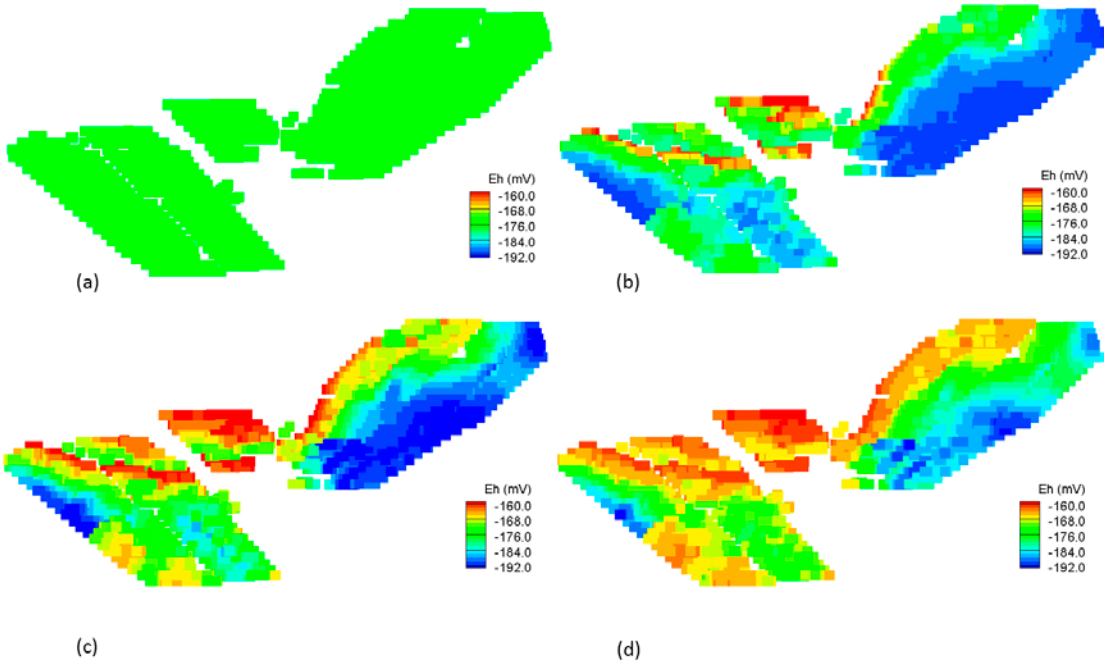

Figure 4-16. *Distribution of Eh at repository depth (a) at the beginning of the simulation, (b) after 1,000 y, (c) after 5,000 y and (d) after 10,000 y (figure taken from Trinchero et al. 2014).*

5 Discussion and conclusions

A numerical methodology for the efficient solution of multicomponent transport problems has been presented. The approach, denoted as FASTREACT, falls within the theory of stochastic-convective models and consists in decoupling a three-dimensional transport problem into a set of independent one-dimensional streamlines. Reference 1D reactive transport simulations are then used to provide time variable concentration distributions at the intersection of the streamlines with given control planes/control volumes.

The proposed methodology is similar to the one denoted as LaSAR-PHREEQC by Malmström et al. (2004). This means that there are no differences between FASTREACT and the LaSAR-PHREEQC approach of Malmström et al. (2004), in terms of principles, potential fields of application, input data that can be handled, or process models that can be used. Instead, FASTREACT should be viewed as tool for modelling reactive transport according to the LaSAR-PHREEQC concept. However, FASTREACT has been developed with safety assessment calculations of radionuclide transport in fractured rock in mind. Therefore, it provides capabilities for handling large amounts of input and output data (e.g. travel time PDFs obtained from particle tracking simulations rather than from pre-defined parametric functions) , such as those arising when modelling multiple realisations of stochastic input parameters. Furthermore, in FASTREACT exchange of mass between a mobile zone (i.e. the fracture) and the matrix can be explicitly accounted for.

One of the key simplifying assumptions of FASTREACT is the neglect of mass exchange between adjacent streamlines (i.e. the neglect of transverse dispersion). This assumption may have important implications in some specific transport configurations where transverse dispersion triggers mixing processes that in turn enhance geochemical reactions. Thus, in order to test the suitability of FASTREACT when applied to a heterogeneous velocity field and to verify the correct implementation of the methodology, a comparison exercise has been carried out.

In this comparison exercise, a reactive transport problem has been solved using both a “standard” Eulerian approach and FASTREACT. The simulations have been carried out over five randomly selected multi-Gaussian fields and the results provided by the two approaches (i.e. breakthrough curves averaged over given control planes) have been compared. The main conclusions can be summarised as follows:

- The computed breakthrough curves (conservative solute) show that the agreement between the two approaches is good for all the considered cases. In some realisations a slight discrepancy is observed which may be attributed to the effect of mixing (not accounted for in FASTREACT).
- The agreement seems to be related to the Peclet number of the problem (i.e. primarily to the effect of transverse local dispersion), such that it is better in the simulations that are “advection-dominated” and slightly poorer for the realisations with comparatively slower velocities.
- The FASTREACT methodology has also been tested using a reactive solute (i.e. Strontium) undergoing ion exchange and precipitation. The resulting average retardation factor of the solute is approximately equal to 1.8. The agreements observed with the reactive solute are not substantially different from those observed for the conservative tracer.
- The computational performance of the two methodologies has been compared. The execution time of the Eulerian simulation depends largely on the average plume velocity while the execution time of FASTREACT is related to the distribution of travel times at the considered control plane. Overall, the execution time of FASTREACT is one order of magnitude lower than that of the Eulerian approach. This difference is expected to increase in more complex three-dimensional systems.

In the second part of the report, we have presented a real-case application where the adoption of FASTREACT has allowed fully coupled reactive transport simulations to be performed at a regional scale and over very large time frames. The model includes the simulation of mass exchange processes between the mobile domain (i.e. fractures and deformation zones) and the immobile domain (i.e. the bedrock between fractures and deformation zones). The results, presented in a summarised form, show that the approach is able to capture the mutual interplay of different processes: advection through the fractures, key geochemical reactions and the buffering effect of the matrix.

References

SKB's (Svensk Kärnbränslehantering AB) publications can be found at www.skb.se/publications.

Abarca E, Carrera J, Sánchez-Vila X, Dentz M, 2007. Anisotropic dispersive Henry problem. Advances in Water Resources 30, 913–926.

Aucour A-M, Tao F-X, Moreira-Turcq P, Seyler P, Sheppard S, Benedetti M F, 2003. The Amazon River: behaviour of metals (Fe, Al, Mn) and dissolved organic matter in the initial mixing at the Rio Negro/Solimões confluence. Chemical Geology 197, 271–285.

Berglund S, Cvetkovic V, 1996. Contaminant displacement in aquifers: coupled effects of flow heterogeneity and nonlinear sorption. Water Resources Research, 23–32.

Bradbury M H, Baeyens B, 2000. A generalised sorption model for the concentration dependent uptake of caesium by argillaceous rocks. Journal of Contaminant Hydrology 42, 141–163.

Brouwer E, Baeyens B, Maes A, Cremers A, 1983. Cesium and rubidium ion equilibria in illite clay. Journal of Physical Chemistry 87, 1213–1219.

Chu M, Kitanidis P K, McCarty P L, 2005. Modeling microbial reactions at the plume fringe subject to transverse mixing in porous media: when can the rates of microbial reaction be assumed to be instantaneous? Water Resources Research 41. doi:10.1029/2004Working Report 003495.

Cirpka O A, Kitanidis P K, 2000. An advective-dispersive stream tube approach for the transfer of conservative-tracer data to reactive transport. Water Resources Research 36, 1209–1220.

Cvetkovic V, Dagan G, 1994. Transport of kinetically sorbing solute by steady random velocity in heterogeneous porous formations. Journal of Fluid Mechanics 265, 189–215.

Dagan G, Cvetkovic V, 1996. Reactive transport and immiscible flow in geological media. I. General theory. Proceedings of the Royal Society of London A 452, 285–301.

Deutsch C L, Journel A G, 1998. GSLIB: Geostatistical Software Library and user's guide. 2nd ed. New York: Oxford University Press.

Fernàndez-Garcia D, Illangasekare T H, Rajaram H, 2005. Differences in the scale dependence of dispersivity and retardation factors estimated from forced-gradient and uniform flow tracer tests in three-dimensional physically and chemically heterogeneous porous media. Water Resources Research 41, W03012. doi:10.1029/2004 Working Report 003125.

Fletcher C A J, 1991. Computational techniques for fluid dynamics. Vol 2, Specific techniques for different flow categories. 2nd ed. New York: Springer.

Gómez-Hernández J J, Wen X-H, 1998. To be or not to be multi-Gaussian? A reflection on stochastic hydrogeology. Advances in Water Resources 21, 47–61.

Grandia F, Sena C, Arcos D, Molinero J, Duro L, Bruno J, 2007. Quantitative assessment of radionuclide retention in the near-surface system at Forsmark. Development of a reactive transport model using Forsmark 1.2 data. SKB R-07-64, Svensk Kärnbränslehantering AB.

Harbaugh A W, Banta E R, Hill M C, McDonald M G, 2000. MODFLOW-2000. The U.S. Geological Survey modular ground-water model – User guide to modularization concepts and the ground-water flow process. Open-File Report 00-92, U.S. Geological Survey, Denver, Colorado.

Herrera P A, Massabó M, Beckie R D, 2009. A meshless method to simulate solute transport in heterogeneous porous media. Advances in Water Resources 32, 413–429.

Kitanidis P K, 1994. The concept of the dilution index. Water Resources Research 30, 2011–2026.

Knutson C E, Werth C J, Valocchi A J, 2005. Pore-scale simulation of biomass growth along the transverse mixing zone of a model two-dimensional porous medium. Water Resources Research 41, W07007. doi:10.1029/2004 Working Report 003459.

Lipson D S, McCray J E, Thyne G D, 2007. Using PHREEQC to simulate solute transport in fractured bedrock. Ground Water 45, 468–472.

Löfman J, Pitkänen P, Mészáros F, Keto V, Ahokas H, 2009. Modelling of groundwater flow and solute transport in Olkiluoto – Update 2008. Posiva Working Report 2009-78, Posiva Oy, Finland.

Löfman J, Poteri A, Pitkänen P, 2010. Modelling of salt water upconing in Olkiluoto. Posiva Working Report 2010-25, Posiva Oy, Finland.

Malmström M E, Destouni G, Martinet P, 2004. Modeling expected solute concentration in randomly heterogeneous flow systems with multicomponent reactions. Environmental Science & Technology 38, 2673–2679.

Malmström M E, Berglund S, Jarsjö J, 2008. Combined effects of spatially variable flow and mineralogy on the attenuation of acid mine drainage in groundwater. Applied Geochemistry 23, 1419–1436.

Oya S, Valocchi A J, 1998. Transport and biodegradation of solutes in stratified aquifers under enhanced in situ bioremediation conditions. Water Resources Research 34, 3323–3334.

Parker J C, van Genuchten M T, 1984. Flux-averaged and volume averaged concentrations in continuum approaches to solute transport. Water Resources Research 20, 866–872.

Parkhurst D L, Appelo C A J, 1999. User's guide to PHREEQC (version 2): a computer program for speciation, batch-reaction, one-dimensional transport, and inverse geochemical calculations. Water-Resources Investigations Report 99-4259, U.S. Geological Survey, Denver, Colorado.

Parkhurst D L, Kipp K L, Engesgaard P, Charlton S R, 2004. PHAST: a program for simulating ground-water flor, solute transport, and multicomponent geochemical reactions. Techniques and Methods 6-A8, U.S. Geological Survey Denver, Colorado.

Piqué A, Grandia F, Sena C, Arcos D, Molinero J, Duro L, Bruno J, 2010. Conceptual and numerical modelling of radionuclide transport in near-surface systems at Forsmark. SR-Site Biosphere. SKB R-10-30, Svensk Kärnbränslehantering AB.

Pitkänen P, Korkealaakso J, Löfman J, Keto V, Lehtinen A, Lindgren S, Ikonen A, Aaltonen I, Koskinen L, Ahokas H, Ahokas T, Karvonen T, 2008. Investigation plan for infiltration experiment in Olkiluoto. Posiva Working Report 2008-53, Posiva Oy, Finland.

Posiva, 2009. Olkiluoto site description 2008. Posiva 2009-01, Posiva Oy, Finland.

Sanford W E, Konikow L F, 1989. Simulation of calcite dissolution and porosity changes in saltwater mixing zones in coastal aquifers. Water Resources Research 25, 655–667.

Shapiro A M, Cvetkovic V D, 1988. Stochastical analysis of solute arrival time in heterogeneous porous media. Water Resources Research 24, 1711–1718.

Simmons C S, Ginn T R, Wood B D, 1995. Stochastic-convective transport with nonlinear reaction: mathematical framework. Water Resources Research 31, 2675–2688.

Tonkin J W, Balistrieri L S, Murray J W, 2002. Modeling metal removal onto natural particles formed during mixing of acid rock drainage with ambient surface water. Environmental Science & Technology 36, 484–492.

Trinchero P, Beckie R, Sanchez-Vila X, Nichol C, 2011. Assessing preferential flow through an unsaturated waste rock pile using spectral analysis. Water Resources Research 47, W07532. doi:10.1029/2010 Working Report 010163.

Trinchero P, Román-Ross G, Maia F, Molinero J, 2014. Posiva Safety Case – Hydrochemical evolution of the Olkiluoto site. Posiva Working Report 2014-09, Posiva Oy, Finland.

Valkiainen M, 1992. Diffusion in the rock matrix – A review of laboratory tests and field studies. Report YJT-92-04, Nuclear Waste Commission of Finnish Power Companies, Finland.

van der Zee S E A T M, Van Riemsdijk W H, 1987. Transport of reactive solute in spatially variable soil systems. Water Resources Research 23, 2059–2069.

van Genuchten M T, Nielsen D R, 1985. On describing and predicting the hydraulic properties of unsaturated soils. Annales Geophysicae 3, 615–628.

Zavala-Sanchez V, Dentz M, Sanchez-Vila X, 2009. Characterization of mixing and spreading in a bounded stratified medium. Advances in Water Resources 32, 635–648.

Zheng C, Wang P, 1999. MT3DMS: a modular three-dimensional multi-species transport model for simulation of advection, dispersion, and chemical reactions of contaminants in groundwater systems. Documentation and user's guide. Contract Report SERDP-99-1, U.S. Army Engineer Research and Development Center, Vicksburg, MS.